



Dynamics of Whitcomb Flats

Grays Harbor



Dynamics of Whitcomb Flats

Gray Harbor

Prepared for:

Port of Grays Harbor in coordination with the Coastal
Communities of Southwest Washington

Prepared by:

Philip D. Osborne, Ph.D.

July 10, 2003



PACIFIC INTERNATIONAL ENGINEERING^{PLLC}
POST OFFICE BOX 1599 • 123 SECOND AVENUE SOUTH • EDMONDS, WASHINGTON • 98020

Table of Contents

1.	Introduction.....	1
1.1	Purpose and Scope.....	1
1.2	Location and Description.....	2
1.3	The Grays Harbor Navigation Project.....	7
1.3.1	History of Maintenance Dredging and Disposal in the Outer Navigation Channel.....	9
2.	Geomorphological Change Analysis.....	17
2.1	Bathymetry and Shoreline Change Analysis.....	17
2.2	Aerial Photograph Analysis of Whitcomb Flat (1960s to present).....	28
3.	Wave Transformation Modeling.....	33
3.1	Sources of Wave Energy at Whitcomb Flat.....	33
3.2	Modeling Assumptions, Grids and Boundary Conditions.....	35
3.3	Selection of Incident Waves for Modeling.....	39
3.4	Wave Height Changes at Whitcomb Flat (1894 to 2002).....	42
4.	Summary and Discussion.....	53
5.	References.....	57

Appendices

Appendix A - Bathymetric Surfaces for Grays Harbor Main Channel
1956 to 2002.

Appendix B - Combinations of Incident Wave Parameters Simulated
with the STWAVE Model.

List of Figures

Figure 1-1	Location of Whitcomb Flats in Grays Harbor	4
Figure 1-2	Provinces of sand deposition in Grays Harbor as described by Scheidegger and Phipps (1976).....	5
Figure 1-3	Map prepared by Captain George Vancouver in 1798 (adapted from Washington State Archives).....	5
Figure 1-4	Map of Grays Harbor in 1841 (adapted from US Department of Commerce archive).....	6
Figure 1-5	Conceptual model of inlet morphology (adapted from Hayes, 1980) applied to Grays Harbor inlet in 1894	6

Figure 1-6. The Grays Harbor Navigation Project (modified from USAED, Seattle, 1989)8

Figure 1-7 Annual maintenance dredging volumes between 1976 and 2002 for the outer navigation channel: Bar Channel (a), Entrance and Point Chehalis Reaches (b), South Reach (c), Crossover Reach (d), and total for the outer reaches (e)13

Figure 1-8. Location of disposal sites in the outer navigation channel, Grays Harbor, Washington (Modified from USAED, Seattle, 1989)15

Figure 2-1 Low water and high water shoreline positions in Grays Harbor entrance for 1862, 1894 and 1900 (top) and 1909, 1921, 1936 (bottom).....20

Figure 2-1 (continued). Low water and high water shoreline positions in Grays Harbor entrance for 1944, 1950, and 1959 (top) and 1965, 1975, 1987 and 2001 (bottom).....21

Figure 2-2 Bathymetry change in Grays Harbor main channel near Whitcomb Flat between 1956 and 200223

Figure 2-3 Bathymetry change in Grays Harbor main channel near Whitcomb Flat between 1956 and 197524

Figure 2-4 Cross-section locations for documenting channel and shoal development and migration between 1956 and 2002.....26

Figure 2-5 Change in bathymetry along cross-section 1 from 1956 to 200226

Figure 2-6 Change in bathymetry along cross-section 2 from 1956 to 200227

Figure 2-7 Change in bathymetry along cross-section 3 from 1956 to 200227

Figure 2-8 Change in bathymetry along cross-section 4 from 1956 to 200228

Figure 2-9 Ortho-rectified photo mosaic of Whitcomb Flat area based on photography acquired in 200129

Figure 2-10 EOW polygons for Whitcomb Flat derived from aerial photographs between 1967 and 200130

Figure 2-11 Migration pattern of the centroid of the Whitcomb Flat EOW polygons between 1990 and 200132

Figure 3-1 Bathymetry grids used for the two-dimensional wave transformation modeling for 1894, 1955, 1965, 1975, 1987, 1993, 1996, and 200237

Figure 3-2 Joint distribution of H_s and T_p for measurements at the Grays Harbor CDIP buoy 3601 between January 1994 and December 2002. Color scale represents number of hours per year.....40

Figure 3-3 Wave rose showing percent frequency of occurrence for all waves in 11.25-deg bands41

Figure 3-4	Wave height (contours) and wave direction (arrows) as simulated by the STWAVE model for incident H_s of 4 m, T_p of 12 sec, and DIR of 270 deg at maximum flood, mhhw, and maximum ebb	43
Figure 3-5	Wave height (contours) and wave direction (arrows) as simulated by the STWAVE model for incident H_s of 8 m, T_p of 16 sec, and DIR of 270 deg at maximum flood current at mid tide, mean higher high water, and maximum ebb current at mid tide	44
Figure 3-6	Location of transect for analysis of spatial and temporal wave height variation.....	46
Figure 3-7	Depth variations along a channel transect for 1894, 1955, and 2002 model grids.....	46
Figure 3-8	Wave height variations along a channel transect for incident waves with H_s of 8 m and T_p of 16 sec.....	47
Figure 3-9	Wave height variations along a channel transect for incident waves with H_s of 8 m, and T_p of 16 sec....	47
Figure 3-10	Wave height (contours) and wave direction (arrows) as simulated by the STWAVE model for high water slack (right: $H_s = 4$ m, $T_p = 12$ sec, DIR = 270 deg; left: $H_s = 8$ m, $T_p = 16$ sec, DIR = 270 deg) on the 1955 bathymetry.....	49
Figure 3-11	Wave height (contours) and wave direction (arrows) as simulated by the STWAVE model for high water slack (left: $H_s = 4$ m, $T_p = 12$ sec, DIR = 270 deg; right: $H_s = 8$ m, $T_p = 16$ sec, DIR = 270 deg) on the 1987 bathymetry	50
Figure 3-12	Wave height (contours) and wave direction (arrows) as simulated by the STWAVE model for high water slack (left: $H_s = 4$ m, $T_p = 12$ sec, DIR = 270 deg; right: $H_s = 8$ m, $T_p = 16$ sec, DIR = 270 deg) on the 2002 bathymetry.....	51
Figure 3-13	Area near Whitcomb Flat for calculating spatially-averaged wave height over time.....	52
Figure 3-14	Time series of spatially-averaged wave heights at Whitcomb Flat simulated with the STWAVE model for two incident conditions	52
Figure A-1	Bathymetric surface for Grays Harbor main channel in 1956. Depths are feet, mllw.	1
Figure A-2	Bathymetric surface for Grays Harbor main channel in 1965. Depths are feet, mllw.	1
Figure A-3	Bathymetric surface for Grays Harbor main channel in 1975. Depths are feet, mllw.	2
Figure A-4	Bathymetric surface for Grays Harbor main channel in 1987. Depths are feet, mllw.	2
Figure A-5	Bathymetric surface for Grays Harbor main channel in 1993. Depths are feet, mllw.	3
Figure A-6	Bathymetric surface for Grays Harbor main channel in 1996. Depths are feet, mllw.	3
Figure A-7	Bathymetric surface for Grays Harbor main channel in 1998. Depths are feet, mllw.	4

Figure A-8 Bathymetric surface for Grays Harbor main channel in 1975. Depths are feet, mllw.4

Figure A-9 Bathymetric surface for Grays Harbor main channel in 2000. Depths are feet, mllw.5

Figure A-10 Bathymetric surface for Grays Harbor main channel in 2001. Depths are feet, mllw.5

Figure A-11 Bathymetric surface for Grays Harbor main channel in 2002. Depths are feet, mllw.6

List of Tables

Table 1-1 Summary of Tidal Datum Planes for Grays Harbor, Washington.....3

Table 1-2 Grays Harbor Navigation Channel Dimensions.....9

Table 1-3 Summary of annual maintenance dredging volumes and decadal statistics (1991-2001) by reach for the outer navigation channel and Crossover Reach, Grays Harbor 12

Table B-1 Combinations of incident wave parameters simulated with the STWAVE model 1

1. Introduction

Pacific International Engineering, ^{PLLC} at the request of, and in coordination with, the Port of Grays Harbor and the Coastal Communities of Southwest Washington, has conducted an analysis of the dynamics of Whitcomb Flat, in Grays Harbor, Washington. The work completed will assist the Port in addressing a request from Washington State Department of Natural Resources (WDNR) to examine the potential for adverse impacts on state-owned aquatic lands caused by the navigation channel of the Grays Harbor and Chehalis River Navigation Project. WDNR raised concerns that increased wave energy stemming from the jetties or wave action from large vessels is exacerbating the migration of Whitcomb Flat and that ongoing navigation in the harbor could decrease the likelihood of the future formation of spits and shoals within the harbor.

1.1 Purpose and Scope

This report documents an analysis of the geomorphic change and inlet processes at and adjacent to Whitcomb Flats in Grays Harbor since jetty construction. The purpose of the analysis is to provide baseline information on physical processes and geomorphology needed to assess potential impacts to Whitcomb Flats by ongoing maintenance of the navigation channel which forms part of the U.S. Army Corps of Engineers (USACE), Grays Harbor and Chehalis River Navigation Project. The information will be of value to assess whether ongoing navigation in the harbor will adversely affect the future formation of spits and shoals within the harbor.

The history of the Grays Harbor and Chehalis River Navigation project is briefly reviewed and the current project is described. Maintenance and new work dredging and disposal activities relevant to sand flat dynamics in the inlet throat are reviewed and analyzed.

Historical bathymetry surveys were analyzed to determine sediment erosion and accretion patterns and trends and to quantify variability in channel and shoal movement adjacent to Whitcomb Flats. Historical aerial photographs of Whitcomb Flats dating back to 1962 were analyzed to quantify shoal migration rates and patterns. Unfortunately, no topographic or bathymetric data were available for the flats themselves. Low water and high water shoreline changes in the inlet throat were described in as much detail as afforded by the available data.

The wave climate at Whitcomb Flat is dominated by storm waves and swell from the Pacific Ocean. Energy from wind-generated waves generated in Grays Harbor and vessel-generated waves are discussed briefly in Section 3 and shown to be insignificant in relation to the contribution from oceanic waves. Therefore, the analysis in this report is focused on ocean wave

processes. The propagation and transformation of ocean waves into Grays Harbor as far east as Whitcomb Flats is analyzed by means of the STeady-state spectral WAVE model (STWAVE) (Resio 1987; Smith et al 2001). Wave transformations are calculated on two-dimensional grids developed from historical bathymetry surveys dating back prior to construction of the entrance jetties. The purpose of the analysis is to examine the long term changes in wave height in relation to engineering modifications in the inlet and morphological changes that have occurred in the inlet and specifically at Whitcomb Flat.

1.2 Location and Description

Whitcomb Flats is a sand flat located in the Grays Harbor estuary within one mile due east of the entrance to Westport Marina and immediately south of the present navigation channel. The entrance to Grays Harbor is approximately 45 miles north of the Columbia River entrance and 110 miles south of the Strait of Juan de Fuca. The main body of Whitcomb Flats is situated near the eastern end of the inlet throat at the confluence of the South Bay tidal channel (a.k.a. Ocosta Channel) and the main tidal channel. Most of Whitcomb Flat is submerged at high tide. Only a small portion remains sub-aerial at high tide (Figure 1-1).

Grays Harbor is one of the largest estuaries in the continental United States. The length of the estuary is approximately 15 miles, with a width of approximately 11 miles (at the widest section), and water surface area ranges from 91 square miles at mean higher high water (mhhw) to 38 square miles at mean lower low water (mllw). Tidal datum planes for Grays Harbor are summarized in Table 1-1. Grays Harbor estuary is a drowned river valley that formed as a consequence of sea level rise following Pleistocene glaciation. The estuary became partially filled during the Holocene with coarse-grained sediment of fluvial and marine origin (Scheidegger and Phipps, 1976; Washington Department of Ecology, 1977; Peterson, Scheidegger and Komar, 1984; Peterson and Phipps, 1992). The sediment infilling process during the Holocene resulted in distinct zones of marine, mixed, and fluvial sediment throughout the estuary. Scheidegger and Phipps (1976) identified sediment distributions from heavy mineral concentrations in 77 surface samples. Two distinct heavy mineral assemblages resulted in the identification of three sand depositional provinces within the estuary (Figure 1-2). Whitcomb Flats is situated entirely within the marine province associated with the entrance area.

**Table 1-1 Summary of Tidal Datum Planes for Grays Harbor, Washington
(Source: Osborne and Arden (2003), Table 2-1)**

Tidal Datum Plane	Elevations in m (ft) Referred to mllw		
	Westport (NGS PID # SD0042)	Point Chehalis ²	Aberdeen ²
Highest Tide (Observed 06/20/1982)	3.35 (11.0)	4.27 ³	4.54 ³
Mean Higher High Water (mhhw)	2.79 (9.16)	2.74	3.08
Mean High Water (mhw)	2.57 (8.43)	2.50	2.87
Mean (Half) Tide Level (mtl)	1.50 (4.91)	1.46	1.66
National Geodetic Vertical Datum 1929 (NGVD29) ¹	1.46 (4.78)		
North American Vertical Datum 1988 (NAVD88) ¹	0.46 (1.51)		
Mean Low Water (mlw)	0.42 (1.39)	0.43	0.46
Mean Lower Low Water (mllw)	0.00 (0.00)	0.00	0.00
Lowest Tide (Observed 06/23/1982)	-0.66 (-2.18)	-1.07 ³	-0.88 ³
Notes: ¹ The NAVD88 and the NGVD 29 elevations related to mllw were computed from Bench Mark, 944 1102 TIDAL 2 1952, at the station; the elevation of mllw to NAVD88 is -1.51 ft. ² USAED. Seattle (1989) ³ Estimated Conversion to National Geodetic Survey (NGS) NAVD88: Subtract 0.66 m (1.51 ft) from the mllw elevation to obtain the NAVD88 elevation			

Prior to jetty construction, there is little information with which to evaluate the dynamics of Whitcomb Flats. A chart prepared by Captain George Vancouver, dated 1798, indicates a large area that was “dry at low water” situated east of the southern barrier (a.k.a. Point Hansen and Point Chehalis) at the confluence of the South Bay Channel and the main entrance channel (Figure 1-3). Figure 1-4 shows

a map of Grays Harbor compiled in 1841 that indicates several isolated shoals east of the inlet throat and extensive shallow areas on the margins of the estuary. The first extensive mapping of the harbor was completed in 1883 by the U.S Coast and Geodetic Survey. These early maps and charts illustrate that Grays Harbor inlet had many of the features typical of the standard conceptual model of tidal inlet morphology (e.g. Hayes, 1980): main ebb channel dominated by ebb-tidal currents, terminal lobe (ebb shoal) where the ebb jet diminishes to allow substantial deposition, marginal flood channels and the updrift and downdrift barriers dominated by flood tidal currents and waves. Figure 1-5 illustrates application of the conceptual model of Hayes applied to Grays Harbor inlet in 1894, a few years prior to jetty construction. This interpretation suggests that Whitcomb Flats originated as part of the flood tidal shoal complex. The flood shoal complex also includes Sand Island shoal on the north side of the main entrance channel. Sediment was originally provided to the flats primarily by flood tidal transport through the marginal flood channels and wave-induced longshore transport along the channel margin bars and barrier spits.

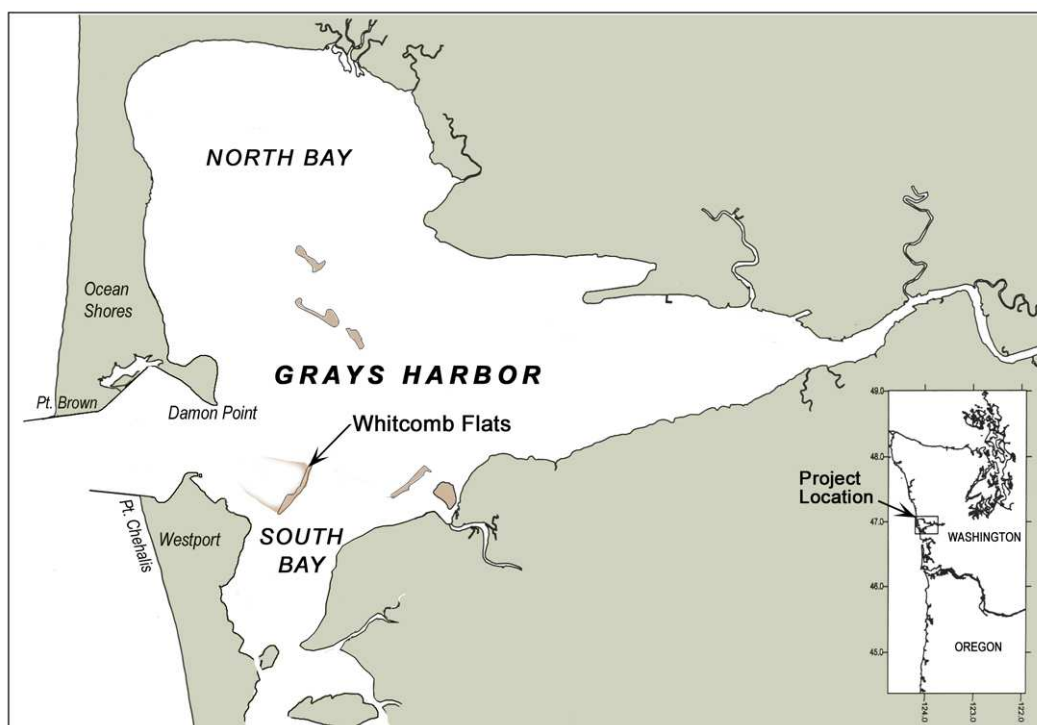


Figure 1-1 Location of Whitcomb Flats in Grays Harbor



Figure 1-2 Provinces of sand deposition in Grays Harbor as described by Scheidegger and Phipps (1976)



Figure 1-3 Map prepared by Captain George Vancouver in 1798 (adapted from Washington State Archives)

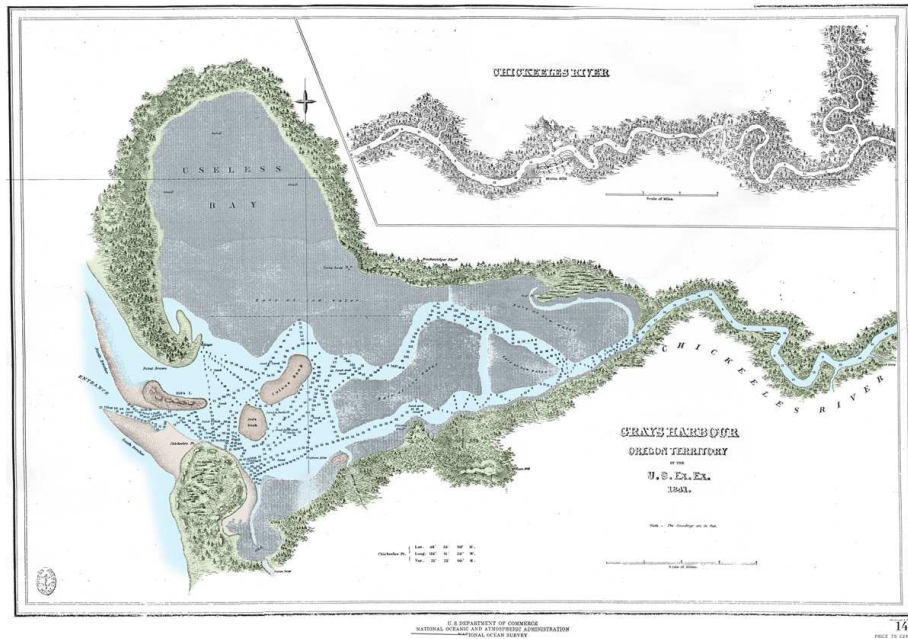


Figure 1-4 Map of Grays Harbor in 1841 (adapted from US Department of Commerce archive)

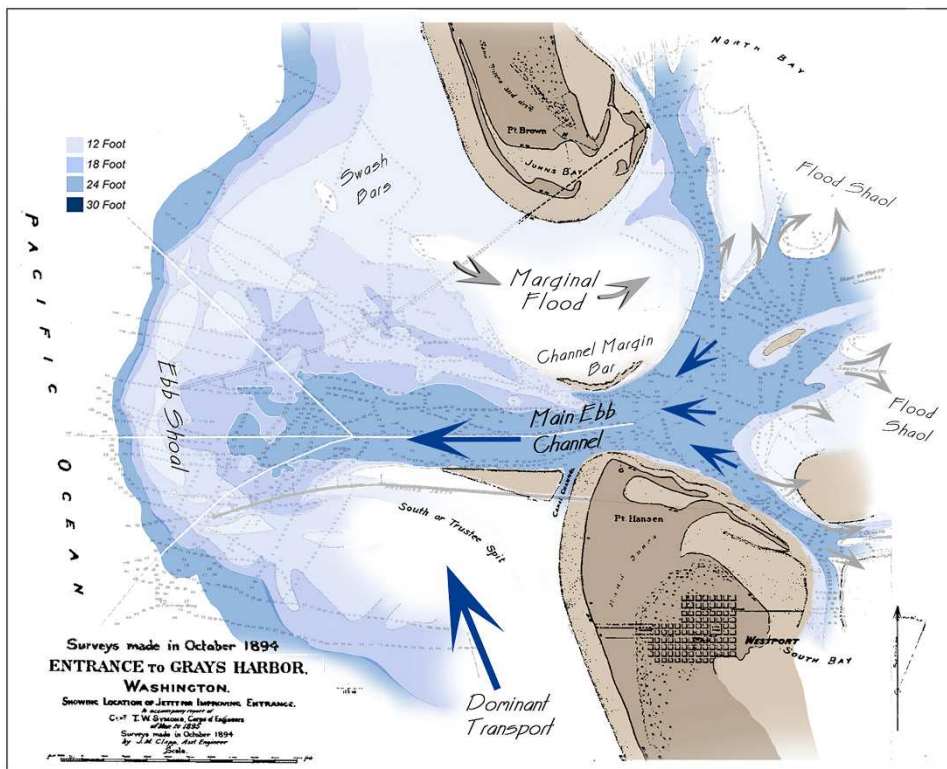


Figure 1-5 Conceptual model of inlet morphology (adapted from Hayes, 1980) applied to Grays Harbor inlet in 1894

1.3 The Grays Harbor Navigation Project

The Grays Harbor Navigation Project is a federally constructed and maintained navigation channel that allows deep-draft shipping through the outer bar, Grays Harbor estuary and the Chehalis River to Cosmopolis. Two jetties that stabilize the harbor entrance are also part of the existing project.

The original project, authorized by Congress through the River and Harbor Act on June 3, 1896, provided for the construction of the South Jetty with a top elevation of +8 ft mllw and a length of 13,734 ft. The South Jetty was completed in 1904. At the time of project development, the predominant littoral drift was thought to be from south to north (USAED, Seattle 1989) and the jetty was constructed with the expectation that it would maintain a bar channel in a stable position. However, soon after South Jetty was constructed, it became clear that the South Jetty alone would not stabilize a deep channel. Therefore, North Jetty authorization was provided through the River and Harbor Act, of March 2, 1907 and was first constructed between 1907 and 1913 to mid-tide elevation along a project length of 16,000 ft. The north jetty was designed to block southward movement of littoral drift and aid in maintaining the entrance channel between the jetties (USAED, Seattle 1973).

The jetties were expected to control northward and southward sediment transport toward the channel, constrain the ebb flow, and scour greater depths across the ebb shoal (USAED, Seattle 1974). The shoal at the unimproved harbor entrance obstructed navigation and was a significant hazard for any type of vessel. The controlling depth on the Outer Bar prior to jetty authorization and construction was 12 to 26 ft mllw.

Although the original navigation project did not specify a depth for the channel over the outer bar, it may be assumed that a depth of at least 24 ft mllw was anticipated (Black 1916). At the time, the project for the inner harbor and Chehalis River provided for a channel 18 ft deep and 200 ft wide from the bay to Cosmopolis (Board of Engineers for Rivers and Harbors 1934). The channel has been redesigned several times, increasing channel depth, width, and length. Currently, the Navigation Channel is approximately 27 miles in total length, extending from the seaward end of the Outer Bar to the lower part of Chehalis River. Figure 1-6 shows the present layout of the Grays Harbor Navigation project including the navigation channel reaches, disposal sites and the other engineering structures including the north and south jetties, south jetty refraction mound, the Point Chehalis groins and revetment. The Navigation Channel consists of several reaches as described in Table 1-2. Channel alignments, depths, and widths in the table correspond to the latest channel improvement project, completed in 1991 under Authorization of Section 202 of the Water Resources Development Act, Public Law 99-662, November, 1986.

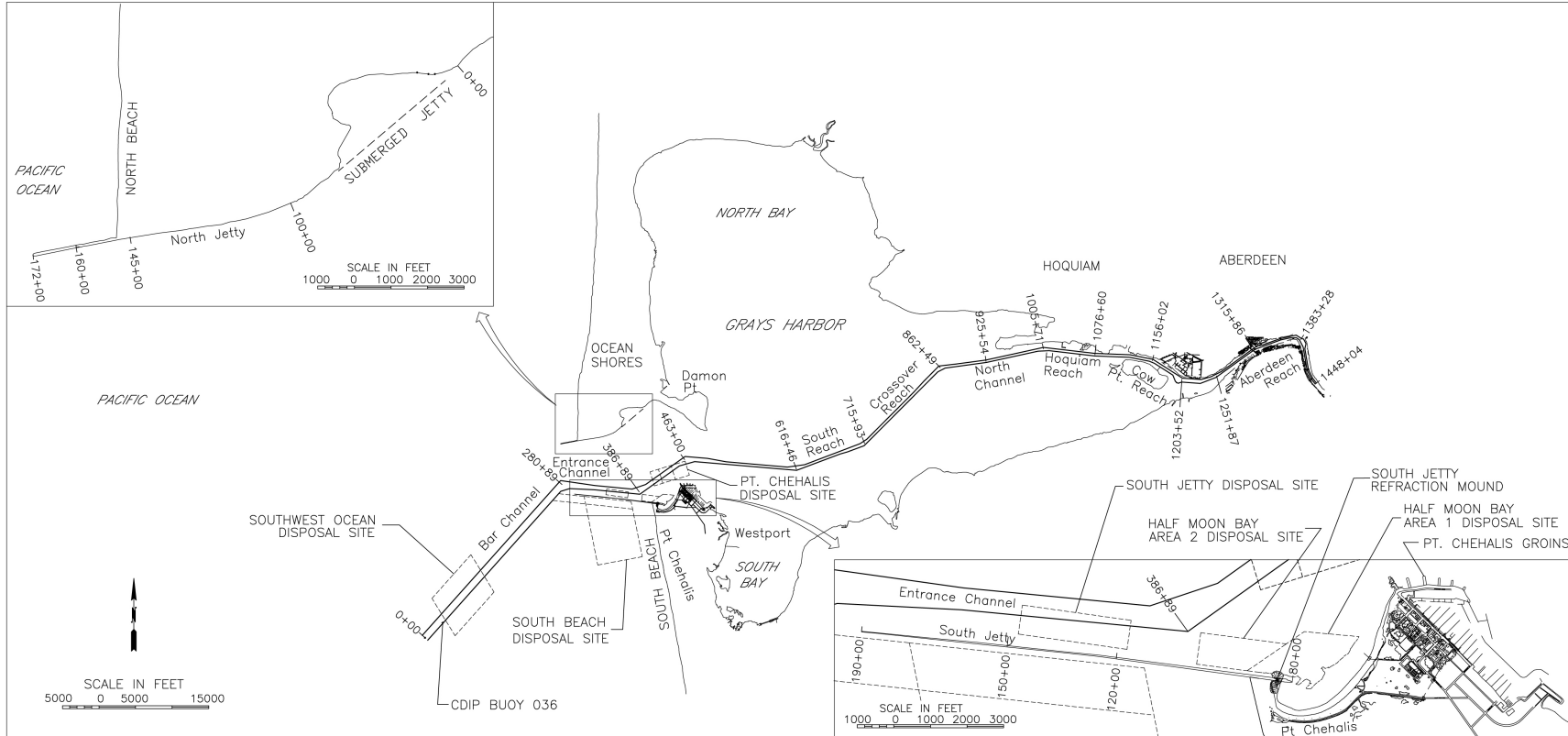


Figure 1-6. The Grays Harbor Navigation Project (modified from USAED, Seattle, 1989)

**Table 1-2 Grays Harbor Navigation Channel Dimensions
(Source: Osborne and Arden (2003), Table 2-1)**

Channel Reach	Stations	Length, (ft)	Channel Depth, (ft)	Channel Width (ft)
Bar Channel	From 0+00 to 280+89	28,089	46	1,000
Entrance Channel	280+89 to 292+89	1,200	46	Varies
Entrance Channel	292+89 to 342+89	5,000	44	600
Entrance Channel	342+89 to 377+89	3,500	42	600
Entrance Channel	377+89 to 386+89	900	40	600
Pt. Chehalis Reach	386+89 to 463+00	7,611	40	600
South Reach	463+00 to 715+93	25,293	36	400
Crossover Channel	715+93 to 862+49	14,656	36	350
North Channel	862+49 to 1005+71	14,322	36	350
Hoquiam Reach	1005+71 to 1156+02	15,031	36	350
Cow Pt. Reach	1156+02 to 1231+50	7,548	36	350
Cow Pt Reach	1231+50 to 1251+87	2,837	32	Varies
Aberdeen Reach	1251 + 87 to 1315 + 86	6,399	32	200
Upper S. Aberdeen Reach	1315 + 86 to 1439 + 65	12,379	32	300

1.3.1 History of Maintenance Dredging and Disposal in the Outer Navigation Channel

The Bar, Entrance, Point Chehalis, and South Reaches, and approximately the outer half of Crossover Reach comprise the outer navigation channel. The inner half of Crossover Reach, North Channel, Hoquiam, Cow Point, and Aberdeen Reaches comprise the inner channel. The material dredged from the outer reaches consists mainly of marine sand deposited by ocean wave and tidal current processes (Figure 1-2). Maintenance dredging and disposal records for the outer navigation channel have been reviewed by the USAED, Seattle (2001), and more recently by Osborne and Arden (2003) as part of North Jetty Performance and Entrance Channel Maintenance study (Kraus and Arden, 2003).

The earliest records of dredging within Grays Harbor date to 1905, when a 200 ft wide channel extending 12 miles downstream from

Cosmopolis was maintained by dredging to a depth of 18 ft mllw (WDOE 1977). Records indicate that regular maintenance dredging of the Bar and Entrance Channels also occurred between 1916 and 1942. During this period, the average volume of maintenance dredging at the Outer Bar and Entrance Channel was approximately 850,000 cu yd/year, all of which was disposed in deep water (below 60 ft mllw) outside the harbor. Between 1916 and 1927, the bar channel was dredged to a depth of 24 ft mllw and from 1928 the dredging continued to a depth of 36 ft mllw. Following rehabilitation of the North Jetty in 1942, maintenance dredging in the Entrance and Bar Channels ceased until 1990 because the improved jetties effectively scoured the entrance area to a navigable depth and prevented marine sediment from remaining in the inlet throat.

No records of maintenance dredging at Crossover Reach and Sand Island Reach prior to 1961 have been found. Between 1961 and 1974, an average of 1,040,000 cu yd per year was dredged from Crossover Reach and Sand Island Reach. In 1978, the Sand Island Reach realignment construction (to become South Reach) was completed because the Sand Island Reach area was shoaling while the South Reach area was eroding. Figure 1-7 shows annual maintenance dredging volumes for the outer reaches of the navigation channel and Crossover Reach. Between 1980 and 1989, following North Jetty rehabilitation in the late 1970s, the annual volumes dredged from Crossover Reach and South Reach were 460,000 and 650,000 cu yd per year, respectively.

The most recent channel deepening improvement project was completed between 1990 and 1991. Channel dimensions were achieved as specified in Table 1-2. South Reach was deepened to 36 feet and widened to 400 ft. Changes to the channel geometry will be further discussed in Section 2.1. Figure 1-7 indicates that approximately 5 million cu yd of sediment were removed from the outer reaches of the navigation channel in 1990 as part of the project. Above average volumes were dredged from the Bar Channel, Entrance, and Point Chehalis Reaches and South Reach during the next three years following the project. Dredging and disposal volumes from maintenance dredging reports and dredging contract documentation for the period 1991 to 2001 were analyzed by Osborne and Arden (2003) to identify trends in sediment distribution along channel reaches since the Navigation Improvement Project. A summary of the analysis is reproduced here. Annual maintenance dredging volumes were estimated from dredging records maintained by the Seattle District. Average annual maintenance dredging volumes for the period 1991 to 2001 for the outer channel reaches are summarized in Table 1-3. Dredging volumes for 2002 are also shown in the table for comparison

with the decadal statistics. Annual dredging volumes depend on the availability of government dredges and funding, as well as the volume of sediment in the channel. Therefore, it is difficult to determine trends from the annual dredged volumes over a period of 12 years.

Maintenance dredging resumed at the Outer Bar, Entrance and Point Chehalis Reaches as a result of the Navigation Improvement Project in the early 1990's. Following the completion of the Navigation Improvement Project, dredging volumes have remained approximately constant at Crossover Reach and decreased at South Reach. On average, approximately 350,000 cu yd per year of sediment have been dredged from South Reach over the last decade in contrast with 650,000 cu yd per year in the previous decade. The decrease in dredging volume at South Reach correlates with ongoing erosion of the south side of the inlet throat area as discussed above in Section 2. On average, approximately 900,000 cu yd per year have been dredged from the combined outer reaches of the navigation channel over the last decade. The volume of sediment dredged from the Bar Channel in 2002 was within the 95 percent confidence intervals of the decadal average value. Volumes dredged from Entrance and Point Chehalis Reaches were above average while volumes dredged from South Reach and Crossover Reach were below average in 2002.

Table 1-3 Summary of annual maintenance dredging volumes and decadal statistics (1991-2001) by reach for the outer navigation channel and Crossover Reach, Grays Harbor

Year	Bar Channel cu yd	Entrance and Point Chehalis Reach, cu yd	South Reach, cu yd	Crossover Reach, cu yd
1991	452000	453000	477000	88000
1992	636000	361000	683000	521000
1993	373000	324000	158000	639000
1994	277000	163000	903600	364000
1995	0	0	332000	469000
1996	0	308000	103600	425000
1997	0	136000	226400	456000
1998	103000	266000	293000	840000
1999	76000	382000	229000	390000
2000	209000	537000	231000	463000
2001	227000	358870	169000	190000
Average annual volume, cu yd/year	214000	299000	346000	440000
Upper 95 percent confidence limit, cu yd/yr	91000	209000	200000	322000
Lower 95 percent confidence limit, cu yd/yr	337000	389000	492000	559000
FY 2002 Actual volumes for comparison, cu yd	144000	605000	136000	22000

Adapted from Osborne and Arden, 2003

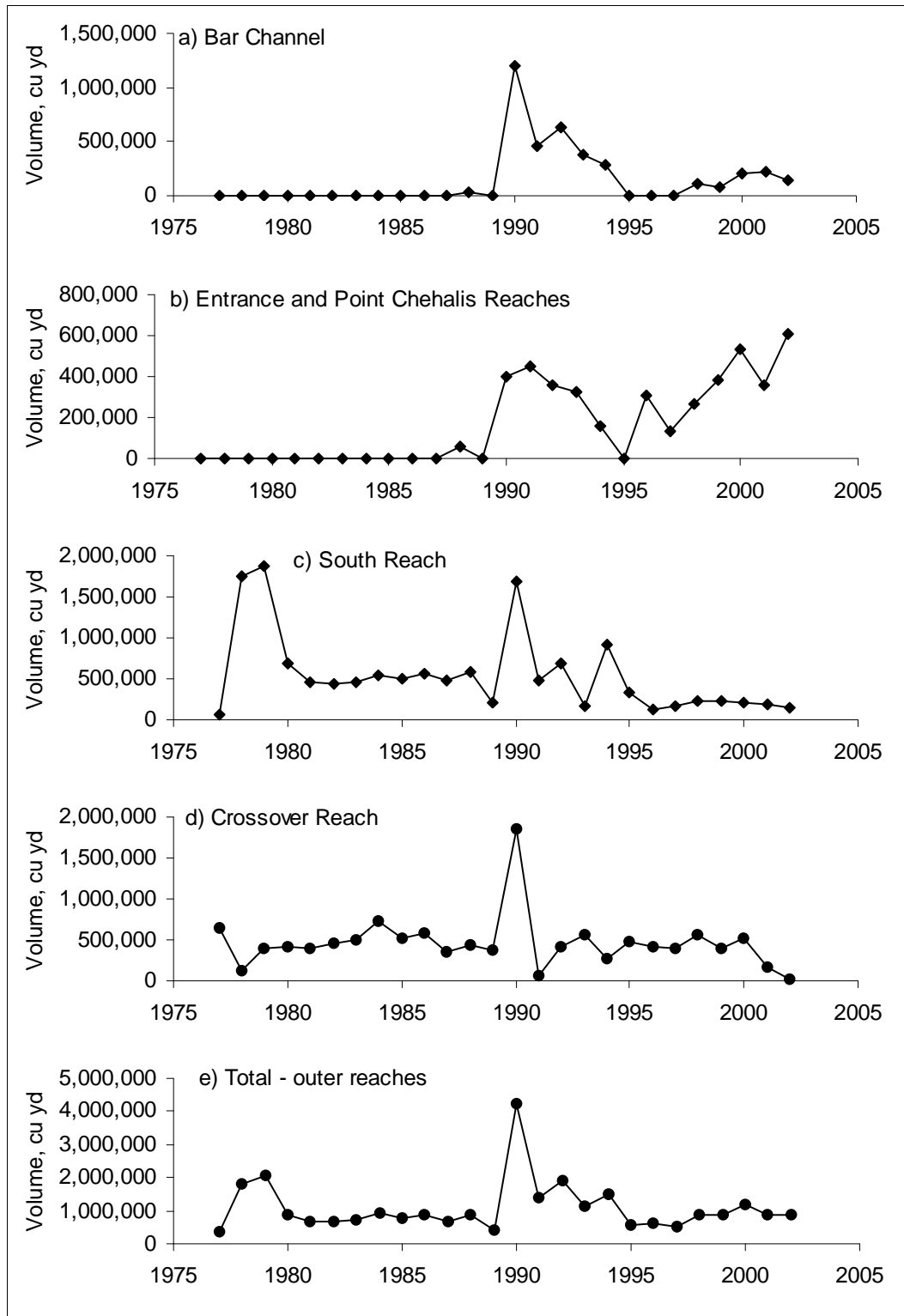


Figure 1-7 Annual maintenance dredging volumes between 1976 and 2002 for the outer navigation channel: Bar Channel (a), Entrance and Point Chehalis Reaches (b), South Reach (c), Crossover Reach (d), and total for the outer reaches (e)

Dredged material from the navigation channels is disposed at six different disposal sites in the Bay and in the open ocean (Osborne and Arden, 2003). The locations of the disposal sites are depicted in Figure 1-8. The volume of dredged material placed at each site is summarized in Table 1-4. Table 1-4 also shows the source of dredged material. Currently, the Seattle District uses disposal sites at Point Chehalis, Half Moon Bay, South Beach, South Jetty, and the Southwest site. Other disposal sites shown on Figure 1-4 are permitted. Selection of specific disposal sites for dredged material disposal is controlled by economic and environmental considerations and an attempt to maximize a beneficial use of dredged material for habitat enhancement and beach restoration projects. For example, sites in Half Moon Bay and Point Chehalis are designated for disposal of dredged material that benefits beach nourishment and shore protection at Point Chehalis and Half Moon Bay. The amount of dredged material placed at the site is controlled by water depth that allows a hopper dredge safe maneuvering during disposal operations. Sites in Half Moon Bay receive dredged material predominately from South Reach, Point Chehalis, and Entrance Reaches, characterized by sand material typical of Half Moon Bay beach sediment (Osborne and Arden, 2003). Sediment pathway analysis (Osborne, Davies and Cialone, 2003) indicates that almost 60 percent of the sediment disposed at Point Chehalis may be transported offshore by the ebb dominant tidal currents. Less than 7 percent is likely to remain in the inlet throat, while the remaining 35 percent is likely to be transported into the inner estuary. The Point Chehalis site is the most likely disposal site to influence sedimentation in the Whitcomb Flat, South Reach and Sand Island areas.

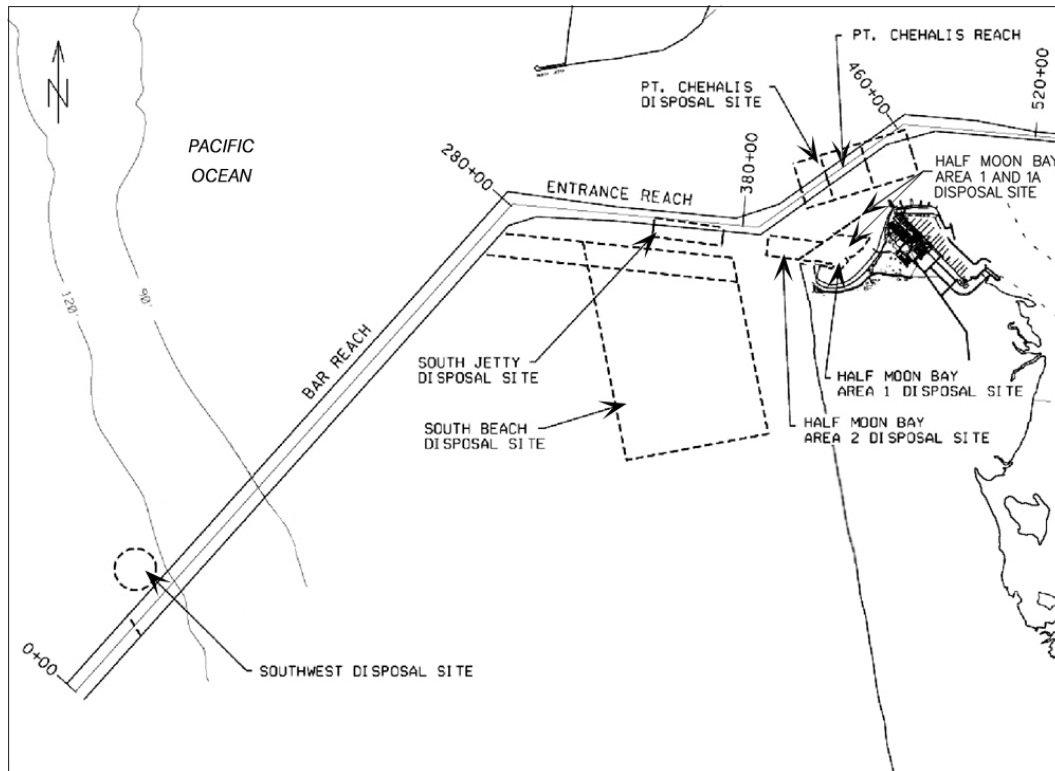


Figure 1-8. Location of disposal sites in the outer navigation channel, Grays Harbor, Washington (Modified from USAED, Seattle, 1989)

Table 1-4 Disposal site annual volumes and sources 1991-2002 (Source: Osborne and Arden, 2003)									
Year	Point Chehalis	South Jetty	Half Moon Bay Nearshore	Half Moon Bay Direct	Westport Fill	Breach Fill	South Beach	SW (Ocean)	Total
1991	710000	1109000	0	0	0	0	0	452000	2271000
1992	990000	1621000	200000	0	0	0	0	637000	3448000
1993	683000	1120000	0	0	0	0	373000	0	2176000
1994	704000	889000	0	0	0	600000	265000	12000	2470000
1995	1181000	392000	0	0	300000	0	0	0	1874000
1996	296000	1674000	275000	0	0	0	0	0	2245000
1997	599000	959000	309000	0	0	0	0	0	1866000
1998	714000	1198000	441000	0	0	0	0	0	2353000
1999	1156000	593000	228000	229000	0	0	76000	0	2283000
2000	956700	1200000	0	0	0	0	0	0	2157000
2001	668000	359000	0	0	0	0	0	227000	1254000
2002	942000	475000	378000	1000	0	135000	75000	69000	2076000
Total volume, cu yd	9600000	11590000	1832000	230000	300000	735000	789000	1397000	26473000
Reaches Dredged	Aberdeen, Cow Point, Cow Point Notch, Inner Crossover, Lower Crossover, Elliot Slough, Hoquiam, Inner Crossover, North Channel, South Reach, Turning Basin, Westport Marina	Aberdeen, Bar, Cow Point, Crossover, Elliot Slough, Entrance, Point Chehalis, Hoquiam, Inner Crossover, North Channel, South Reach	Entrance, South	Entrance, South	South	Entrance, South	Bar	Bar	

2. Geomorphological Change Analysis

The most significant recent geomorphic changes (last 200-500 years) in Grays Harbor are those associated with the construction of jetties at the entrance (USAED, Seattle 1974,1989; Burch and Sherwood 1992; Buijsman et al. 2003; Byrnes and Baker, 2003). Jetty construction in the early 1900s was undertaken to improve channel navigability. The structures imposed substantial influence on estuarine hydrography and channel characteristics, creating a self-scouring inlet that has moved the crest of the offshore bar (ebb-tidal shoal) seaward into deeper water, caused significant sand deposition along the beaches north and south of the harbor, and resulted in accretion of spits and shoals in the entrance region. The geomorphic evolution of the entrance to Grays Harbor since jetty construction has been evaluated by bathymetric change analysis (e.g. Committee on Tidal Hydraulics 1967; Burch and Sherwood, 1992; Byrnes et al, 2003) of annual condition surveys conducted by the USAED, Seattle and shoreline change analysis (e.g. Phipps and Smith, 1978; Burch and Sherwood, 1992; Buijsman et al 2003) derived from aerial photography and historical maps and charts. The annual condition surveys are conducted by hydrographic surveying and do not normally extend into water depths less than approximately 15 to 20 ft. Although the survey data do not reveal the dynamics of sand flat migration, they provide information on the channel dynamics adjacent to Whitcomb Flats. Previous analyses of Grays Harbor are reviewed in section 2.1 and bathymetry changes since the 1950s in the area adjacent to Whitcomb Flat are analyzed in more detail as part of this study. Migration of Whitcomb Flat is examined in section 2.2 by analysis of aerial photographs acquired between 1962 and 2001 made available by the USAED, Seattle and WDNR.

2.1 Bathymetry and Shoreline Change Analysis

Construction of the jetties at the entrance to Grays Harbor between 1898 and 1916 resulted in large changes to the inlet throat, the ebb-tidal shoal and the adjacent beaches. These changes have been documented and summarized by a number of previous studies including: Committee on Tidal Hydraulics (1967), Burch and Sherwood (1992), Kaminsky et al (1999), Byrnes and Baker (2003), Byrnes, Baker, and Kraus (2003), Buijsman et al (2003). Construction of the entrance jetties stabilized the entrance by confining flows in and out of the estuary and blocking littoral drift from shoaling the navigation channel. The studies showed that the inlet channel deepened and the ebb-tidal shoal migrated into deeper water. Between 1900 and 1990, the entrance region eroded at a rate of about 380,000 cy/year (Burch and Sherwood, 1992).

Buijsman et al (2003) and Byrnes et al (2003) present shoreline positions from NOS-T sheets and aerial photographs that indicate that beaches north and south of the inlet accreted rapidly following initial jetty construction. However, deterioration of the jetties in the 1920s and 1930s correlates with retreat of the beaches and accretion of inner harbor spits (Damon Point and

Point Hansen). Following rehabilitation of the jetties in the 1940s, the beaches once again accreted and the inner harbor spits and shoals eroded. The response of the beaches and shoals to the rehabilitation in the 1960s and 1970s has been less obvious. Buijsman et al (2003) summarized three possible reasons for the lack of shoreline response:

1. The rehabilitation projects in the 1960s and 1970s were of smaller scale than the previous rehabilitation in the 1940s
2. The length of the north jetty was not changed in the 1975 rehabilitation
3. Deepening of the seafloor may have permitted larger waves to break nearshore, thereby reducing the capacity of the jetties to hold sand.

Figure 2-1 shows the changes in the mllw position and average high water shoreline positions, respectively, on the north and south sides of the inlet entrance since 1862. The shorelines were compiled by the Washington Department of Ecology (WDOE), and by Byrnes and Baker (2003) and include data from Seattle District field surveys, interpreted shorelines from aerial photography, and shorelines derived from USC & GS topographic sheets.

Prior to jetty construction, well-developed sand spits were present on the north and south barriers at Grays Harbor inlet. Wave-induced longshore sediment transport contributed to the growth and development of the inlet spits and delivered littoral sediments to the tidal channels at the distal ends of the spits and together with tidal currents supplied sediment to Whitcomb Flat and other parts of the flood shoal.

Analysis of shoreline positions indicates that significant changes have occurred on both the north and south side of the inlet entrance since jetty construction. The shoreline north and east of the south jetty receded during the construction of the south jetty and for a short time thereafter, see also USAED, Seattle 1965; Osborne et al. 2003a. However, spit recovery and development occurred north and east of the south jetty as the south jetty deteriorated beginning shortly after construction. Shoreline positions from 1909 indicate incipient growth of what is now Point Chehalis. With continued deterioration of the jetty, increasing amounts of sediment entered the inlet from the south and accreted on Point Chehalis. The mllw shorelines in Figure 2-1 indicate significant shoal accumulation in the Whitcomb Flat area by the early to mid 1940s. Following reconstruction of the south jetty to a top elevation of +20 ft mllw in 1939, sediment supply to Point Chehalis and Whitcomb Flat was significantly reduced. Erosion of Point Chehalis recommenced at the eastern terminus of the jetty, initiating the formation of Half Moon Bay in 1946. Point Chehalis revetment and groins were constructed in the period 1950 to 1956 to stabilize the shoreline in that area. Since that time, Half Moon Bay has continued to erode. A detailed analysis

of sediment transport pathways in Half Moon Bay (Osborne et al. 2003a, b, c) including long term and detailed morphological change analysis, shoreline change analysis, detailed field measurements of waves, currents, and sediment transport, and numerical simulations of waves, currents, and sediment transport, indicates that most sediment eroded from Half Moon Bay is now transported westward out of the inlet by the ebb dominant tidal currents in that region of the inlet. The presence of the Point Chehalis groins, the South Bay tidal channel and the relatively deep water just north of Point Chehalis preclude any significant supply of littoral sediment to the east on the south side of the inlet entrance since the mid 1950s.

On the north side of the inlet, Damon Point originated as a result of spit accretion on the south side of the north jetty following initial construction of the jetty in 1916, as sand that had accumulated to the north of the jetty was transported through and over the northeastern extension of the jetty. The initial growth of Damon Point correlates with subsidence and deterioration of the north jetty that allowed sand from the littoral system to bypass north jetty and feed the spit. As shown in Figure 2-1, growth of the spit continued until the early 1940s. The north jetty was rehabilitated to +20 ft mllw in 1942, and this effectively blocked sand transport from north beach to Damon Point. The reduction in sediment supply caused the spit to breach and decrease in size until approximately 1950. By the 1950s, sand bypassing of north jetty had once again increased to a point where the spit had reformed and began to grow again. During this time period, the spit also migrated eastward along the north jetty, reaching its present position in the late 1960s (Figure 2-1). Since then, the spit has continued to grow mainly at the distal subaqueous portion to the south and east. Implications of recent growth of Damon Point to channel evolution and Whitcomb Flat are examined in more detail below.

Although the historical shorelines compiled by WDOE are useful for the interpretation of medium to long term changes at Damon Point, Point Chehalis, and Half Moon Bay, documentation of historical shoreline position at Whitcomb Flat is incomplete in the WDOE compilation. This deficiency is redressed in Section 2.2.

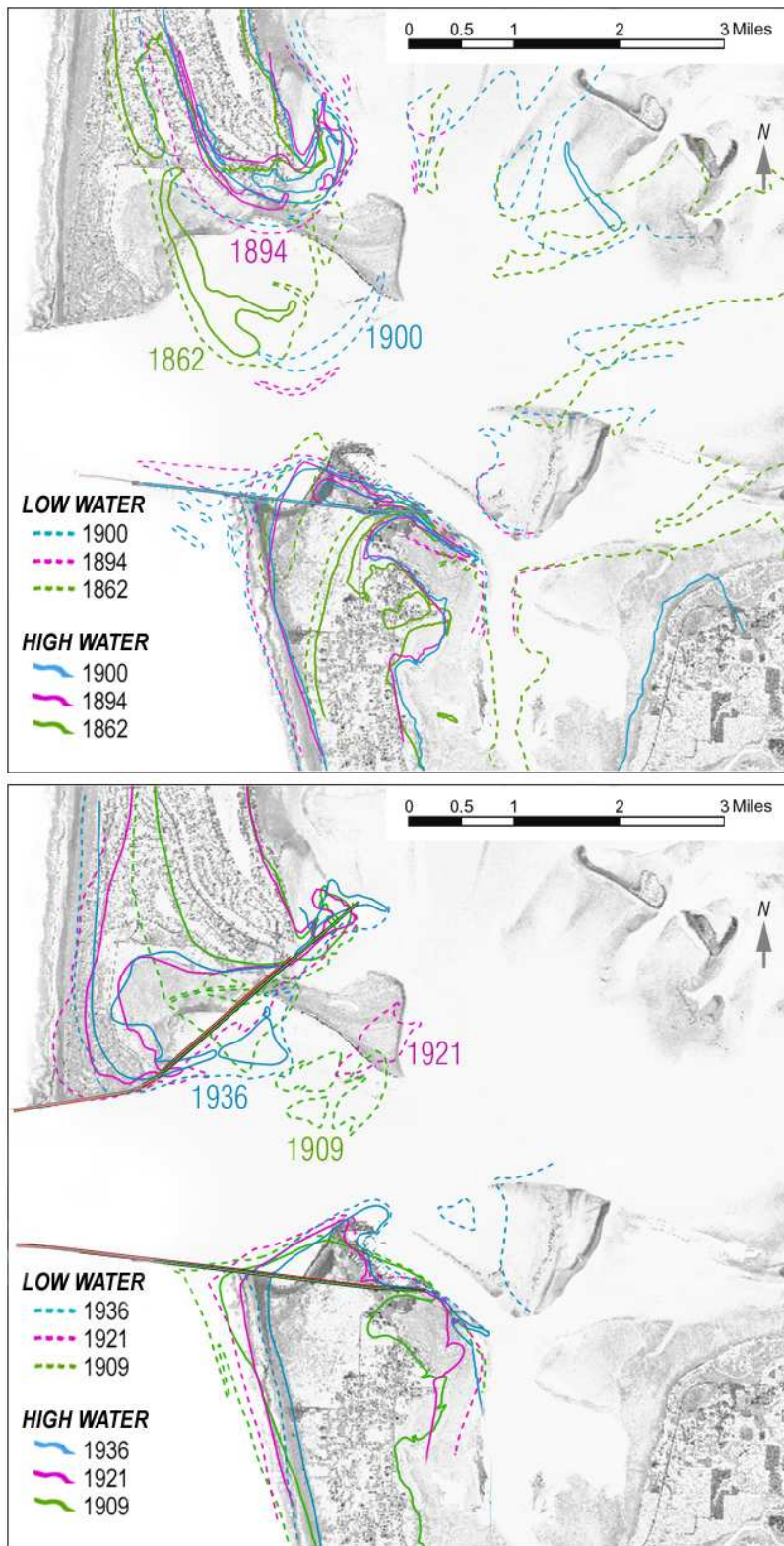


Figure 2-1 Low water and high water shoreline positions in Grays Harbor entrance for 1862, 1894 and 1900 (top) and 1909, 1921, 1936 (bottom)

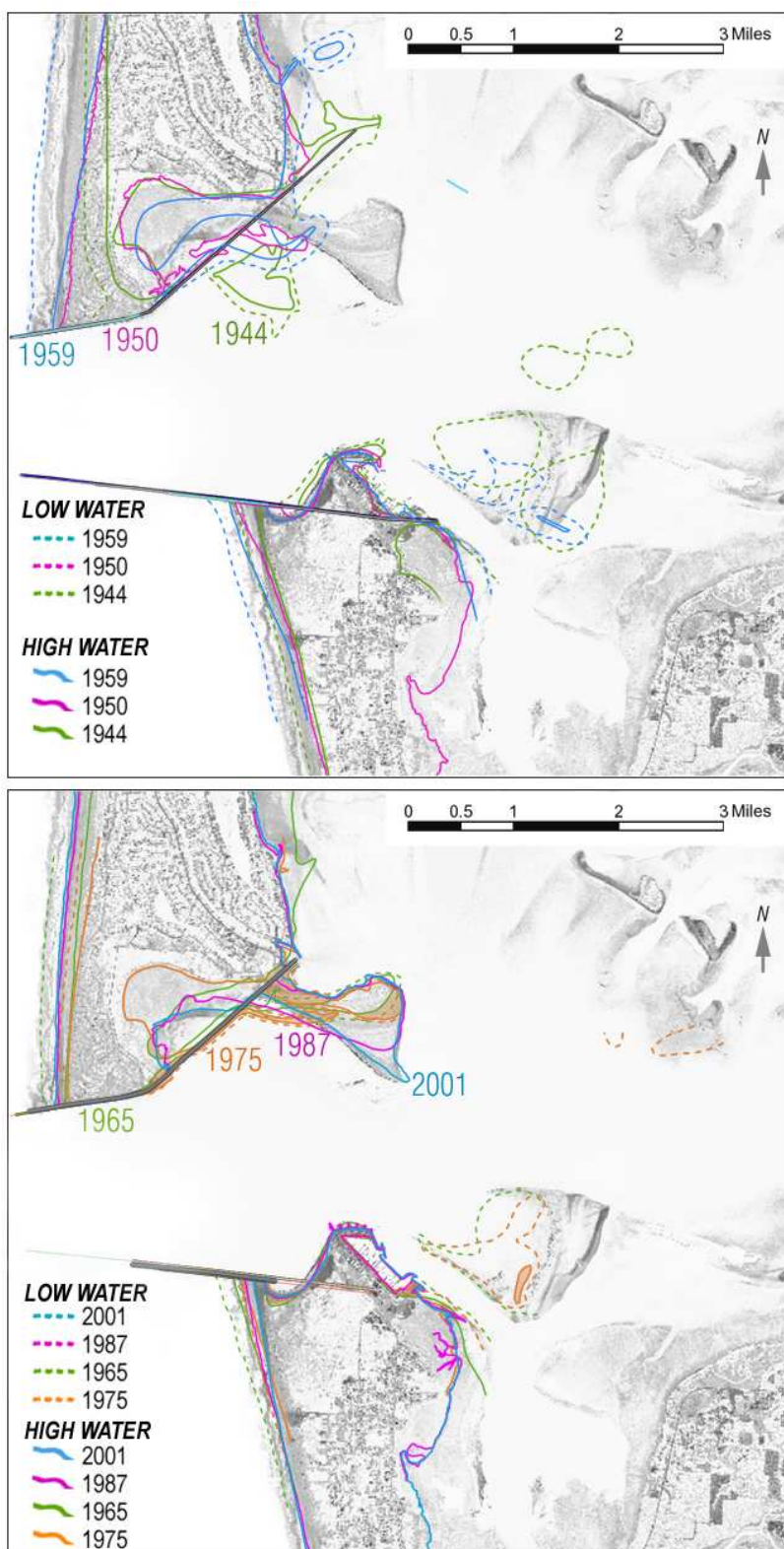


Figure 2-1 (continued). Low water and high water shoreline positions in Grays Harbor entrance for 1944, 1950, and 1959 (top) and 1965, 1975, 1987 and 2001 (bottom)

Analysis of the bathymetry change in the main channel between Westport and Damon Point and extending east between Sand Island Shoal and Whitcomb Flat has been conducted for this study. Bathymetric surfaces for the period 1956 to 2002 derived from annual hydrographic surveys by the USAED, Seattle are provided in Appendix A. Figure 2-2 shows the difference between the bathymetric surfaces derived from the 1956 and 2002 surveys. The change surface and individual bathymetric surfaces indicate that there has been accretion at the southeast end of Damon Point and erosion immediately south of the accretion. This pattern of accretion and erosion indicates that the main channel has shifted laterally to the south over this period of time. According to the sediment budget analysis conducted by Byrnes and Baker (2003), approximately 19×10^6 cubic yards of sediment deposition has occurred on a large subaqueous spit south and west of Damon Point between 1956 and 2002. Byrnes and Baker note that the rate of deposition in this area has been approximately constant since 1954 with accumulation of 480,000 cu yd/year from 1954 to 1987 and 508,000 cu yd/year from 1987 to 2002. The large volume of net accretion on the southeast end of Damon Point over time has created a significant increase in hydraulic resistance in the main channel that has forced the channel to deepen and move to the south. The change in tidal hydraulics and shifting of the channel to the south contributes to conditions that favor deposition on the north side of the main channel and erosion on the south side of the main channel east of Damon Point. The bathymetry change analysis confirms that net accretion has occurred on the north side of the channel (formerly Sand Island Reach) and this has been offset by erosion on the south side of the channel (South Reach) just north of Whitcomb Flat. The sediment budget by Byrnes and Baker (2003) indicates a net accretion of 13.5×10^6 cubic yards in the northern half of the channel south of Sand Island Shoal between 1956 and 2002. An area of net accretion is also evident in Figure 2-2 to the south side of the navigation channel near Point Chehalis. Accretion in this area results from a combination of disposal of dredged sediment and migration of sand waves to the southwest in the inlet throat. The sand waves have developed as a result of strong ebb tidal currents and the hydraulics created by the deep scour that has developed just south of Damon Point.

The greatest change in the inlet entrance and largest transport rates have occurred in the inlet throat which includes the South Reach area. According to the sediment budget analysis by Byrnes and Baker (2003), approximately 35 million cu yd were eroded from the inlet throat between 1987 and 2002, or approximately 2.3 million cu yd per year. Between 1955 and 2002, approximately 75 million cu yd were eroded from the inlet throat or approximately 1.9 million cu yd per year. Byrnes and Baker correlate erosion losses from the inlet throat with seaward transport across the ebb shoal and deposition in the offshore zone outside of Grays Harbor in response to inlet hydraulics. As indicated in Figure 2-2, a significant proportion of the erosion

occurred immediately to the south of Damon Point and north of the navigation channel, where scour of up to 60 ft has occurred (1 ft per yr). Scour depths in the South Reach area over this period average 20 to 30 ft (0.5 ft per yr).

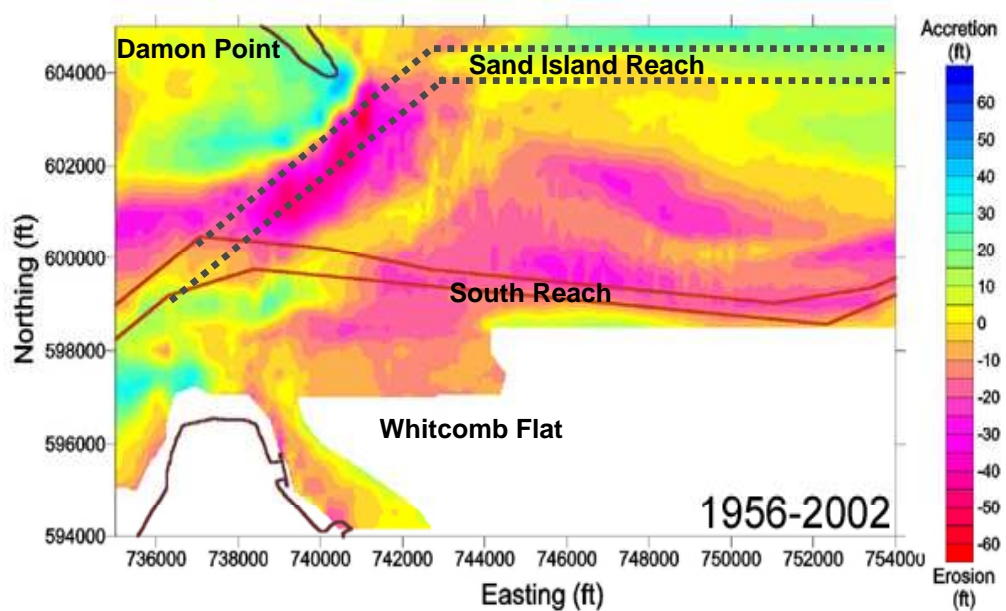


Figure 2-2 Bathymetry change in Grays Harbor main channel near Whitcomb Flat between 1956 and 2002

Figure 2-3 shows the difference between the bathymetric surfaces derived from the 1956 and 1975 surveys during the two decades prior to realignment of the navigation channel from Sand Island Reach to South Reach. The difference map indicates that accretion was occurring in the Sand Island Reach, concurrent with erosion north of Whitcomb Flat and scouring at the end of Damon Point.

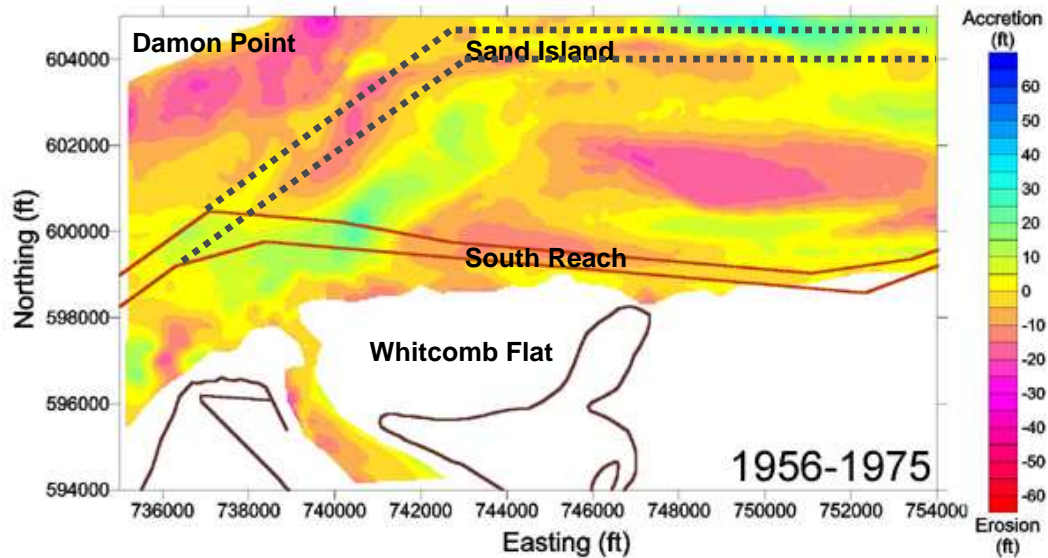


Figure 2-3 Bathymetry change in Grays Harbor main channel near Whitcomb Flat between 1956 and 1975

Cross sections of the main channel area were developed to further document the temporal evolution of the channel and shoals between 1956 and 2002 (Figure 2-4). Cross-section 1 (Figure 2-5), represents the evolution of the main channel across the western end of Whitcomb Flat to the present tip of Damon Point. Between the 1950s and mid 1990s the northern and middle segments deepened rapidly from approximately 30 ft, mllw to more than 90 ft, mllw. The northernmost segment has accreted significantly in the last decade as a result of the southeastward growth of Damon Point. The southern segments of the cross-section have also eroded but at a slower rate.

Cross-sections 2 through 4 (Figure 2-6 through 2-8) document the evolution of the channel between Whitcomb Flat and Sand island Shoal. The cross-sections reveal that scour dominated the southern half of the inlet throat between 1956 and 1987. In 1956, the navigation channel cut is evident in the north half of cross-sections 3 and 4. Over the next two decades, this area was dominated by net accretion while erosion was occurring in the south half of the main channel. The pattern of accretion on the north side of the channel and erosion on the south side during this period led to the realignment of the navigation channel from Sand Island Reach to South Reach in 1978, as dredging volumes in Sand Island Reach had become unmanageable.

From 1987 to 2002, the rate of erosion in this area decreased relative to previous decades. In 1990, the South Reach of the navigation channel was deepened to 36 ft and widened to 400 ft as part of the Navigation Channel

Improvement Project (USAED, Seattle 1989). The bathymetry analysis indicates that at cross-sections 2 and 3 the depth at mid-channel increased by approximately 5 to 7 ft and by less than 2 ft at cross-section 4. The cross-sections indicate that the southern side slope of the channel (between depths of 20 ft and 35 ft) migrated southward at rates of 10 to 15 m/yr between 1965 and 1987. The rate of southward migration of the channel side slope has decreased since 1987.

The bathymetry analysis suggests that the channel relocation in the late 1970s coincided with a period of ongoing relatively rapid southward migration and deepening of the channel which had persisted for at least the previous decade (1965 to 1975) and which continued until the mid 1980s. It is therefore difficult to distinguish the impact of the channel relocation project and dredging from the larger scale morphological changes that were occurring in that part of the inlet throat. Similarly, the deepening and widening project in 1990 caused only a relatively minor increase in overall depth (generally less than 5 to 7 ft) and width of the channel in relation to the larger scale erosion of the throat. It is possible that the channel relocation, dredging, and deepening and widening projects have reinforced the larger scale and longer term system response through positive feedback adding to the overall increase in channel depth, width and tidal flow in this area. However, it is worth noting that the channel position has been relatively stable at depths between 20 and 40 ft for the last decade and a half.

Dredging records available from the Seattle District indicate that an average of 1,040,000 cu yd/year was dredged from the Crossover Reach and Sand Island Reach. The bathymetry analysis, together with the shoreline change patterns discussed above, suggest that much of the erosion and accretion in the South Reach area of the inlet throat was forced by the larger scale changes in tidal hydraulics brought about by the large net accretion occurring at Damon Point that had begun in the previous two decades. In general, the hydrographic surveys conducted by the USAED, Seattle District do not extend into water depths less than 15 to 20 ft, mllw and no sub-aerial topographic surveys of Whitcomb Flat were readily available for analysis in this study. Therefore, it is not possible to analyze the temporal changes in inter-tidal bathymetry, sub-aerial topography, and sub-aerial and sub-aqueous shoal volumes in this report. A limited analysis of the position and shape of the subaerial portion of Whitcomb Flat can be conducted based on aerial photographs since the 1960s. This analysis is presented and the results are discussed in Section 2.2.

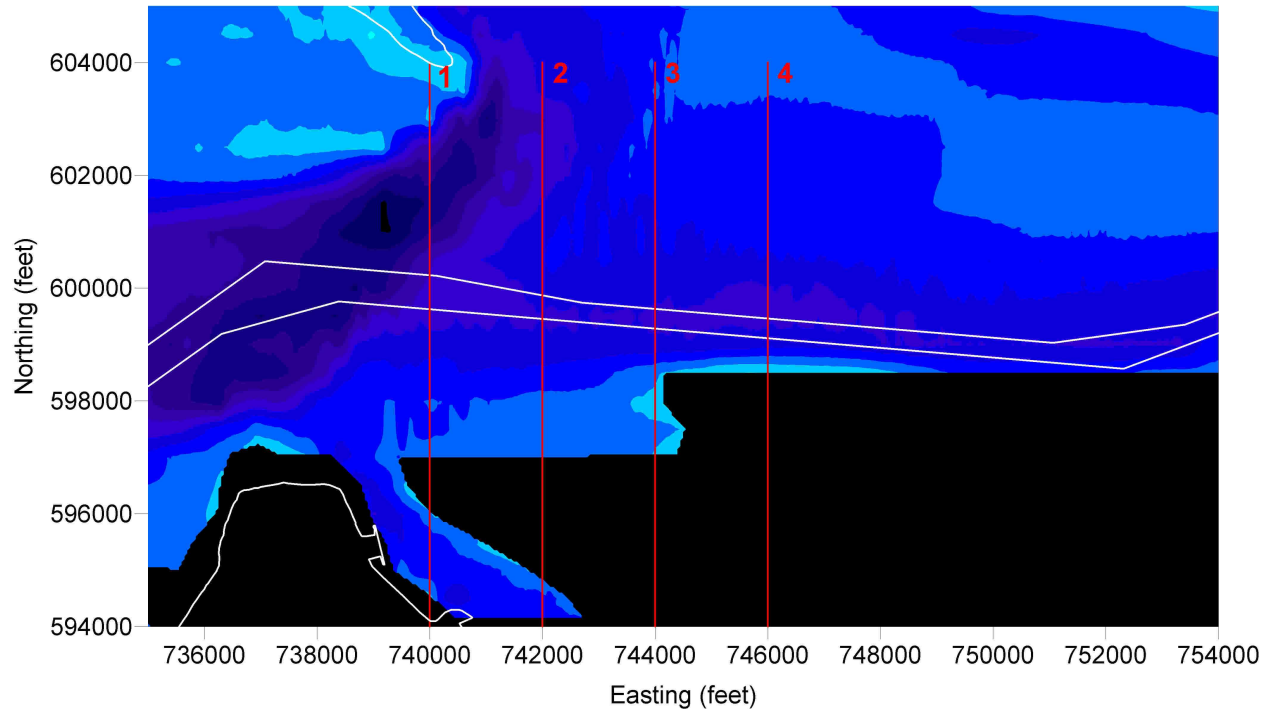


Figure 2-4 Cross-section locations for documenting channel and shoal development and migration between 1956 and 2002

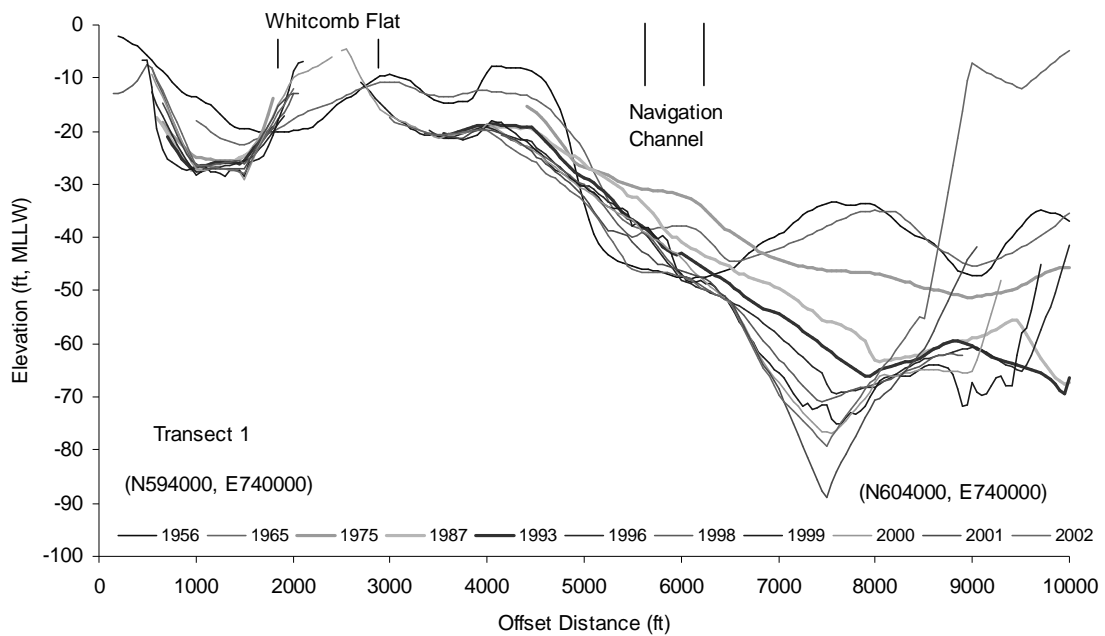


Figure 2-5 Change in bathymetry along cross-section 1 from 1956 to 2002

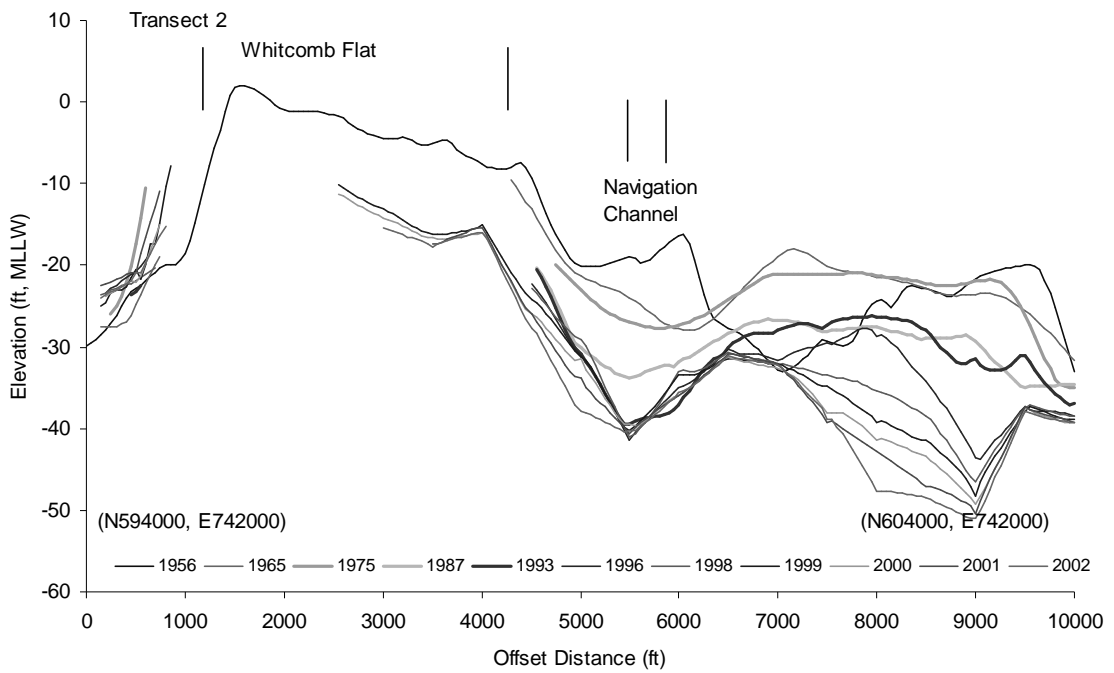


Figure 2-6 Change in bathymetry along cross-section 2 from 1956 to 2002

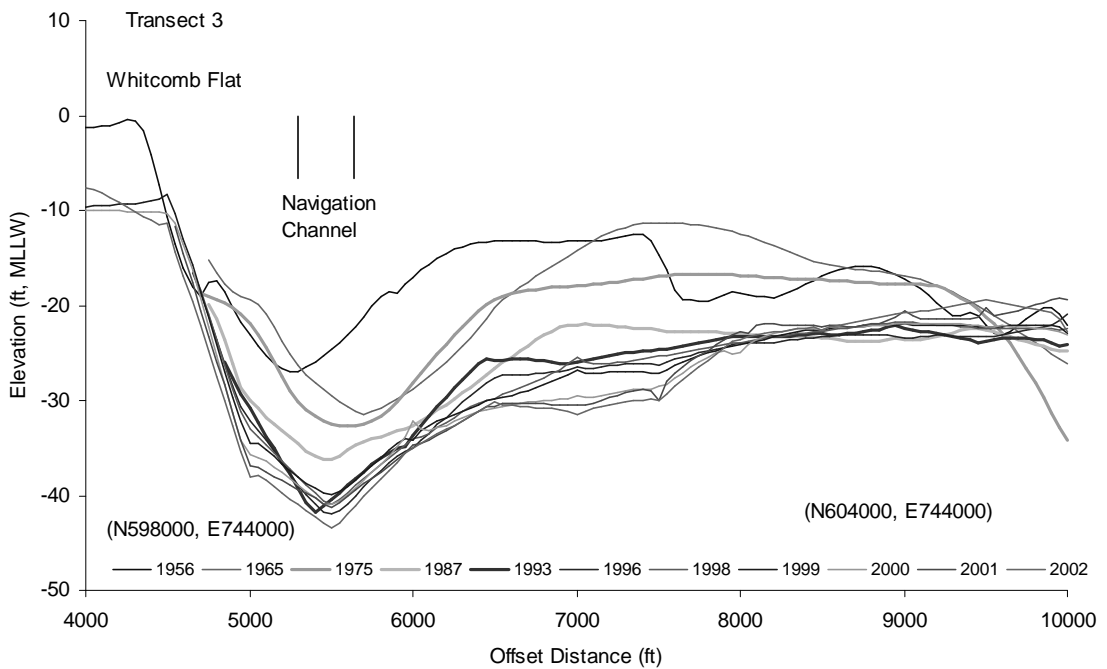


Figure 2-7 Change in bathymetry along cross-section 3 from 1956 to 2002

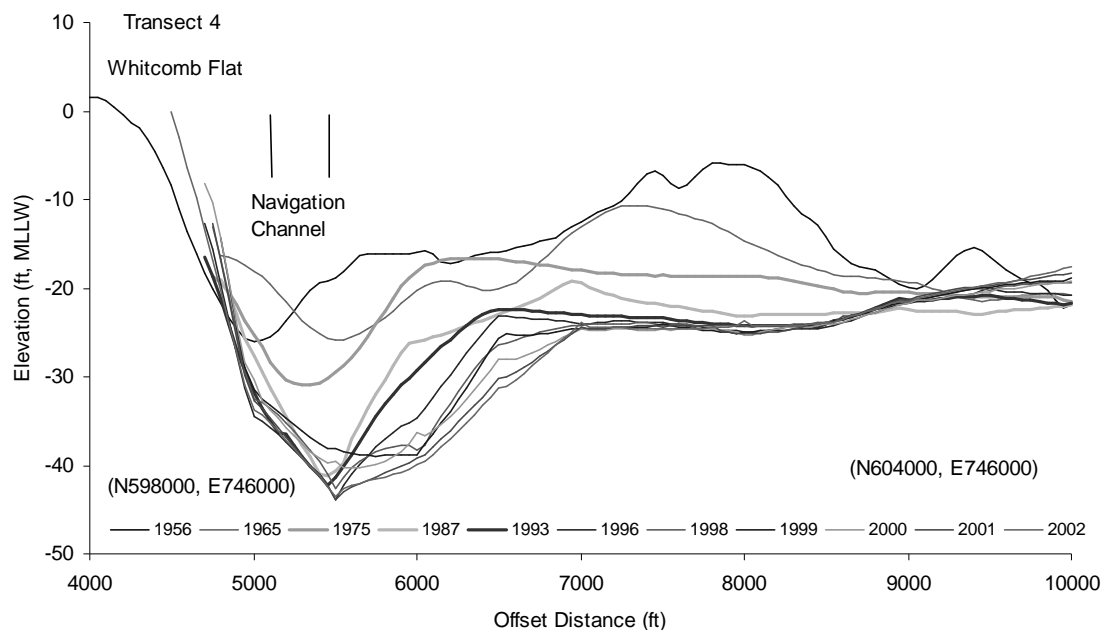


Figure 2-8 Change in bathymetry along cross-section 4 from 1956 to 2002

2.2 Aerial Photograph Analysis of Whitcomb Flat (1960s to present)

The analysis includes comparison of edge of water (EOW) position time series derived from ortho-rectified aerial photographs. EOW positions for Whitcomb Flat were digitized from ortho-photo mosaics for the years 1967, 1977, 1985, 1997, 1998, 1999, 2000, 2001 and 2002. The aerial photography was acquired from the photo archives of the Operation and Maintenance Section of the USAED, Seattle and from the Resource Mapping Photo and Map Sales at Department of Natural Resources. Original photographs covering the area of interest were reproduced at a scale of approximately 1:12000 and were digitized at 600 dots per in., ortho-rectified and arranged in mosaics using the PCI-Geomatica Ortho-Engine software.

A network of Ground Control Points (GCP) for the images was developed by a Real Time Kinematic Global Position System (RTK GPS) survey conducted in January 2003. The RTK-GPS survey obtained spatial coordinates (Easting, Northing and Elevation) of objects or locations that were easily identifiable in the photographs. Typically, seven GCPs were used in each photograph. Also, at least seven tie points, or points common to each photograph for which spatial coordinates are unknown, were identified in the photos. The GCPs and tie points were incorporated in the process of rectification and the creation of the photo mosaics. Camera focal length, and fiducial marks were also incorporated in the rectification process. Root-mean square (rms) error in horizontal pixel position of the ortho-rectified photographs was approximately

2.4 pixels, with pixel resolution typically 0.61 m. RMS errors of less than 2 m were considered acceptable. Figure 2-9 shows the photo mosaic for the 2001 photo sequence.

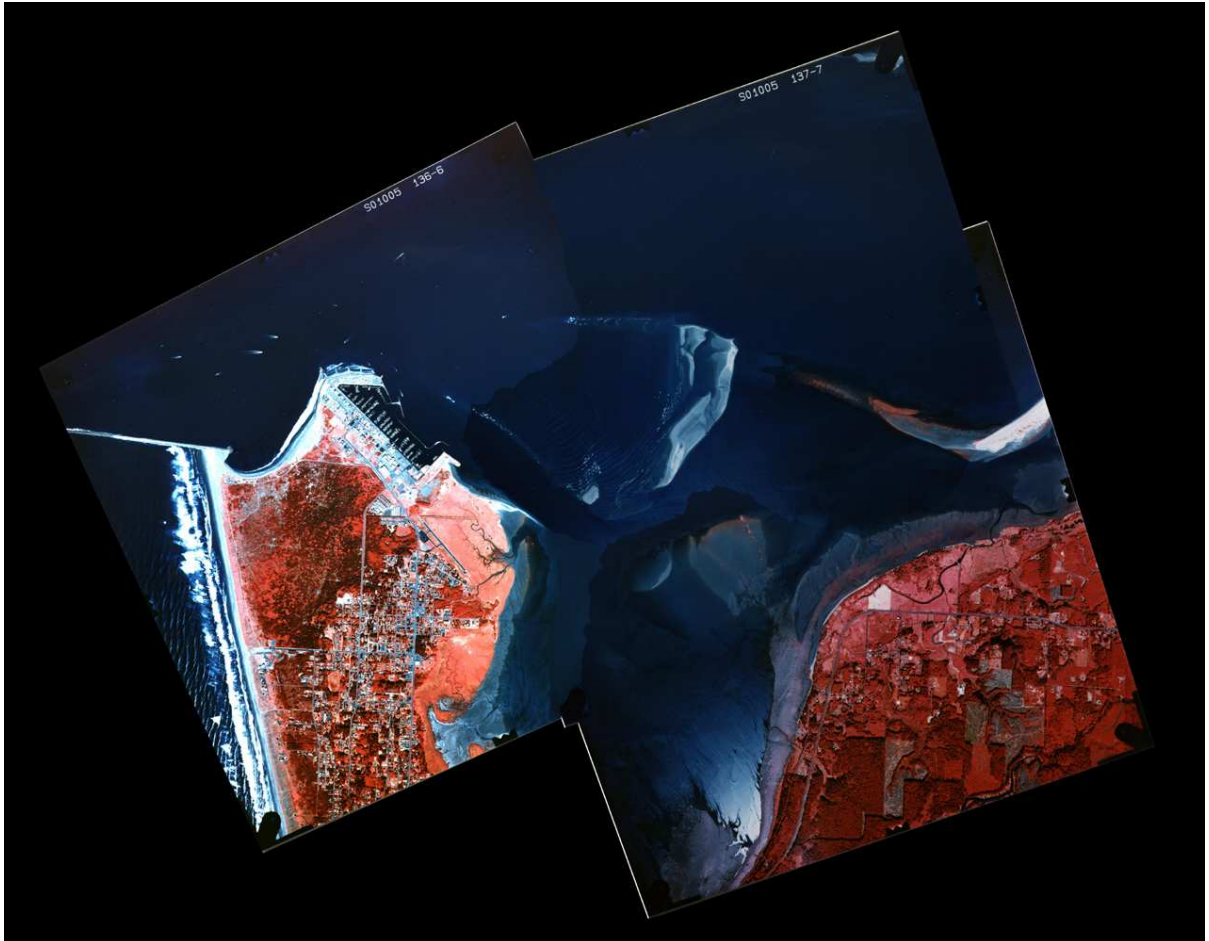


Figure 2-9 Ortho-rectified photo mosaic of Whitcomb Flat area based on photography acquired in 2001

The EOW feature was digitized to create polygons of the approximate supra-tidal portions of Whitcomb Flat using Autocad software. The EOW is an interpreted feature derived from the aerial photography that is based on the contrast between water (dark) and sand flat (light) and represents the shoreline position at the time of the photograph. The interpretation was done by eye, by zooming into the area of interest; no ground truth of the technique was possible.

The sequence of polygons derived from interpretation of the EOW is shown in Figure 2-10. The polygons indicate that Whitcomb Flat has migrated eastward since 1967. The long axis of Whitcomb Flat has been oriented northeast-southwest since the 1960s and the long axis length has remained relatively unchanged over this period of time. The aerial photo mosaic shown in Figure

2-10 indicates that trailing spits have developed westward from the ends of the long axis of the flats along the channel margins. Wave crests of ocean swell are clearly visible between the trailing spits indicating the presents of a ramp-like shoal reminiscent of a flood shoal ramp (e.g. Hayes, 1980).

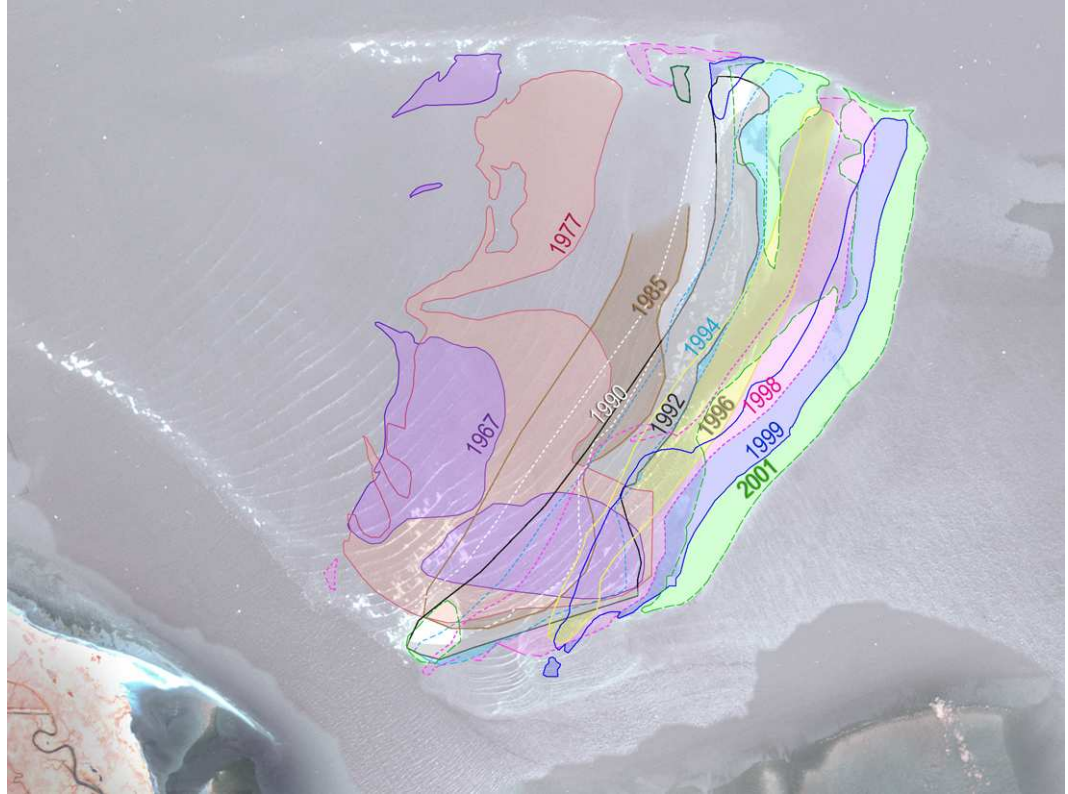


Figure 2-10 EOW polygons for Whitcomb Flat derived from aerial photographs between 1967 and 2001

To minimize the uncertainty associated with temporal (tidal phase) variability in EOW position and total interpretive errors of this feature, horizontal migration of Whitcomb Flat was determined from the centre of mass or centroid of each EOW polygon in the photo time series using the MASSPROP routine in Autocad. The centroid was considered a more robust indicator of the position of Whitcomb Flat than the interpreted position of the EOW at the time of the photograph. The pattern of migration of the centroid (Figure 2-11) indicates that Whitcomb Flat has migrated steadily eastward in the past 34 years. The centroid position for 1967 was computed in two ways: i) including all EOW polygons derived from the 1967 photograph (centroid connected by a solid line in Figure 2-11); ii) excluding the southern-most EOW polygon with an east-west long axis (centroid connected by a dashed line in Figure 2-11). The net distance between the centroids for 1967 and 2001 is 1041 to 1135 m, indicating an average net rate of migration of 30 to 32 m per year over 35 years. Figure 2-12 shows the migration rate of the Whitcomb Flat EOW centroid for intervals between 1967 and 2001. From 1967 to 1977, the

Whitcomb Flat EOW centroid migrated between 180 and 238 m at an average rate of 16 to 22 m per year. Between 1977 and 1990 the EOW centroid migrated a further 213 m at a rate of 15 m per year. Between 1990 and 2001, the centroid migrated 736 m at a rate of 73 m per year. The centroid migration data indicate a marked increase in the rate of migration over the past decade with the highest rates occurring since 1998.

The dominant forcing mechanisms that could account for the morphological evolution, and in particular, the eastward migration of Whitcomb Flat include ocean waves, tidal currents and possibly eolian transport. Circulation modeling of Grays Harbor inlet incorporating tidal forcing (e.g. Cialone et al 2002) and direct field measurements using tripods and vessel-mounted acoustic Doppler profiling current meters (e.g. Osborne et al. 2003) indicates that the inlet throat and the Ocosta Channel are both strongly ebb-dominated. It is therefore unlikely that the eastward migration of the sand flat can be explained by tidal current transport of marine sands. The development of the westward trailing spits is more likely associated with ebb-dominant tidal transport. Although eolian transport by prevailing westerly winds may contribute to eastward migration of the sand flat, the variation of the wind climate over the last decade does not explain the temporal variation in migration rates described above and wind transport is likely to be relatively unimportant considering the relatively small sub-aerial portion of the spit exposed for any significant portion of the tidal cycle. A more plausible hypothesis regarding the eastward migration of the sand flat is that storm waves and swell from the Pacific Ocean and associated high water levels during storms result in overtopping of the sand flat promoting eastward transport of sediment. The spatial and temporal variation of waves entering Grays Harbor and reaching Whitcomb Flat is evaluated in Section 3.

It seems likely that the increase in eastward migration of the sub-aerial portion of Whitcomb Flat is non-linearly related to increases in wave height through sediment transport at this location since the late 1970s. Eastward migration of the crest of the sand flat would likely increase rapidly as the incidence of overtopping increases and as the percentage of a tidal cycle increases during which wave overtopping occurs. Overtopping events will correlate with periods of super elevation of the water surface that are a direct function of offshore incident wave height (Osborne, 2003). It is also possible that dredging and channel deepening have contributed indirectly to the increase in the migration rate of the flat during the last decade through a local increase in depth which in turn has permitted more wave energy to reach Whitcomb Flat.



Figure 2-11 Migration pattern of the centroid of the Whitcomb Flat EOW polygons between 1990 and 2001

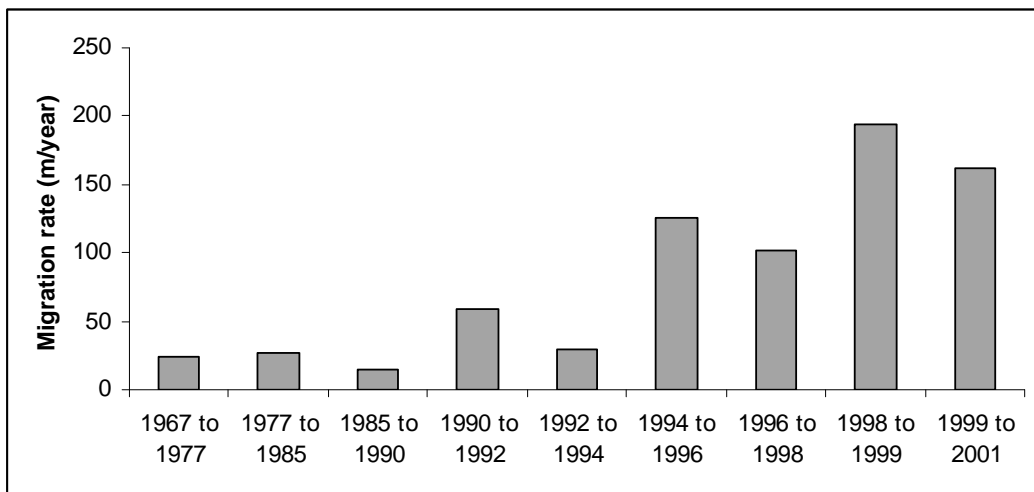


Figure 2-12 Migration rate of the Whitcomb Flat EOW centroid between 1967 and 2001

3. Wave Transformation Modeling

Waves are a primary mechanism controlling gross and net sediment transport in the channels and on the shoals of tidal inlets such as Grays Harbor. Waves are responsible for the generation of steady cross-shore and longshore currents, long-period (infragravity) waves, and water level shifts at the shoreline, the combination of which may result in episodes of erosion and accretion.

This section of the report outlines numerical modeling and the analysis of modeling results that were conducted to evaluate ocean waves and the changes in wave height at Whitcomb Flat. A wave transformation model was established for Grays Harbor entrance extending east to Whitcomb Flat. The purpose of the wave modeling is to gain insight regarding coastal processes and changes in the coastal process regime that might explain the migration patterns observed in Whitcomb Flat.

3.1 Sources of Wave Energy at Whitcomb Flat

Surface gravity waves with periods between 2 and 30 sec arriving at Whitcomb Flat and expending energy in sediment transport may be derived from several sources, including:

- Wind-generated waves and swell from the Pacific Ocean
- Local wind waves generated in Grays Harbor
- Vessel generated waves

The wave climate of the northeastern Pacific Ocean is considered a high energy wave climate. Deep-water significant wave heights, H_s , on the Washington Coast are smallest (< 2.0 m) on average between May and August (late spring to summer), reaching a minimum in July or August. Monthly average wave heights increase between August and November and reach a maximum in December. Average monthly H_s in winter range between 3.6 to 3.8 m in the northern portion of the eastern north Pacific that includes Washington State. Spectral peak wave periods, T_p , exhibit a similar seasonal variation to H_s , averaging less than 10 sec in summer months and increasing to more than 12 sec in winter months. Clearly ocean waves potentially represent a significant portion of the local wave energy spectrum. The transformation of ocean wave energy to Whitcomb flat is discussed and analyzed further in Sections 3.2 to 3.4.

The height and period of local wind waves generated in Grays Harbor are determined by the wind speed, the fetch length, water depth, and the wind duration at a given wind speed. Fetch lengths are determined by harbor geometry but also by tidal phase because of the large expanses of tidal flats in the inner estuary, which become exposed at low water. The maximum unrestricted fetch for waves generated inside the harbor at high tide at

Whitcomb Flat is approximately 7 to 8 nautical miles to the north and the east at high water. The fetch to the north is reduced to 3 to 4 miles at low water. Table 3-1 summarizes predicted spectral wave heights (H_{m0}) and periods (T_p) for a reasonable range of wind speeds for Grays Harbor, assuming the maximum fetch for Whitcomb Flat, fully developed conditions, and an average depth along the entire fetch of 15 ft. These assumptions are conservative and therefore the predictions represent a worst case situation for Grays Harbor. The predictions are based on the shallow water fetch-limited wave growth equations outlined in the USACE Coastal Engineering Manual (EM 1110-2-1100 (Part II) which are also considered conservative. The results of the analysis indicate that under most wind and tide conditions at Grays Harbor, locally generated wind waves are short period (less than 3 sec) and do not exceed 0.5 m in height. This analysis suggests that locally generated wind waves do not represent a significant contribution to the sediment transport potential at Whitcomb Flat.

Table 3-1. Predicted locally generated wind wave parameters for Whitcomb Flat

Beaufort Specification	Wind speed at 10 m (mph)	H_{m0} (m)	T_p (s)
Light breeze	5	0.08	1.2
Gentle breeze	10	0.24	2.0
Moderate breeze	15	0.38	2.4
Fresh breeze	20	0.53	2.7
Strong breeze	25	0.67	3.0
Near gale	30	0.80	3.3
Gale	35	0.93	3.5
Strong gale	45	1.17	3.8

See text for assumptions and methods

Vessel generated waves may arise from recreational vessels, commercial fishing vessels and commercial freight carriers calling at the Port of Grays Harbor. Vessel generated wave heights depend on the distance from sailing line, vessel type, size, draft, speed, load and load distribution and depth of water. Wave periods depend only on vessel speed and water depth. The design vessel for the 1991 Navigation Channel Improvement Project was a timber carrier with 625 ft length, 100 ft beam, and 37 ft draft. The largest vessel recorded to have called at the Port of Grays Harbor had a dry weight tonnage of 50,250 tons, a 686 ft length, 100 ft beam, and 39.8 ft draft.

Wakes heights and periods for the design vessel were developed for Whitcomb Flat using the PIANC (1987) empirical formulae (see Sorensen, 1997 for a summary), the Shipwave model by Weggel and Sorensen (1984), and PI Engineering experience with wake measurements from a range of vessels types and sizes in a number of projects. Wake predictions assumed a design vessel traveling in the navigation channel at a distance of 1000 ft from

Whitcomb Flat with maximum speed of 15 knots and an average water depth of 40 feet. The empirical predictions indicate that vessel wake heights would rarely exceed 0.5 m with periods on the order of 5 sec at Whitcomb Flat.

3.2 Modeling Assumptions, Grids and Boundary Conditions

The STeady-state spectral WAVE model (STWAVE) (Resio 1987; Smith et al 2001) was applied to compute nearshore wave propagation and transformation to Grays Harbor. STWAVE is a steady-state, finite-difference model for near-coast, time-independent spectral wave energy propagation, based on a simplified form of the spectral balance equation. The model assumes:

Only wave energy directed into the computational grid is significant, i.e., wave energy not directed into the grid is neglected

Wave conditions vary slowly enough that the variation of waves at a given point over time may be neglected relative to the time required for waves to pass across the computational grid.

The assumptions underlying STWAVE include:

- Mild bottom slope and negligible wave reflection
- Spatially homogeneous offshore wave conditions
- Steady-state waves, currents and winds
- Linear refraction and shoaling
- Depth-uniform current (if applied)
- Negligible bottom friction
- Linear radiation stress

STWAVE is a finite difference model that calculates wave parameters (wave height, peak period, wave direction, and radiation stresses) at all grid points.

Basic input requirements include:

- Local coordinate system in which the x-axis runs in the cross-shore direction and the y-axis is parallel to the shoreline
- Bathymetry grid (including grid dimensions, grid cell size, and an azimuth orientation of the local coordinate system)
- Incident height, frequency, and direction of waves on the offshore boundary
- Tide elevation

The wave model requires a computational bathymetric grid to transform waves from the offshore boundary at approximately 45 m depth to the inner

harbor. STWAVE requires Cartesian model grids that have square cells. Grids were generated by first using the commercial contouring software Surfer to create interpolated bathymetry plots for the years 1894, 1955, 1965, 1975, 1987, 1993, 1996, and 2002. The contoured bathymetry plots were then transformed into STWAVE depth model grids with the 2002 orientation of the shoreline used as the landward boundary. The grids for each year are shown in Figure 3-1.

Grid cells of 50 m were used, the grid origin is located at easting 214795.1100 m and northing 166589.7634 m Washington State Plane, Zone 4602 (South) NAD83. The grid contains 174344 cells (296 x 589) and covers an area of 435 square kilometers (168 square miles).

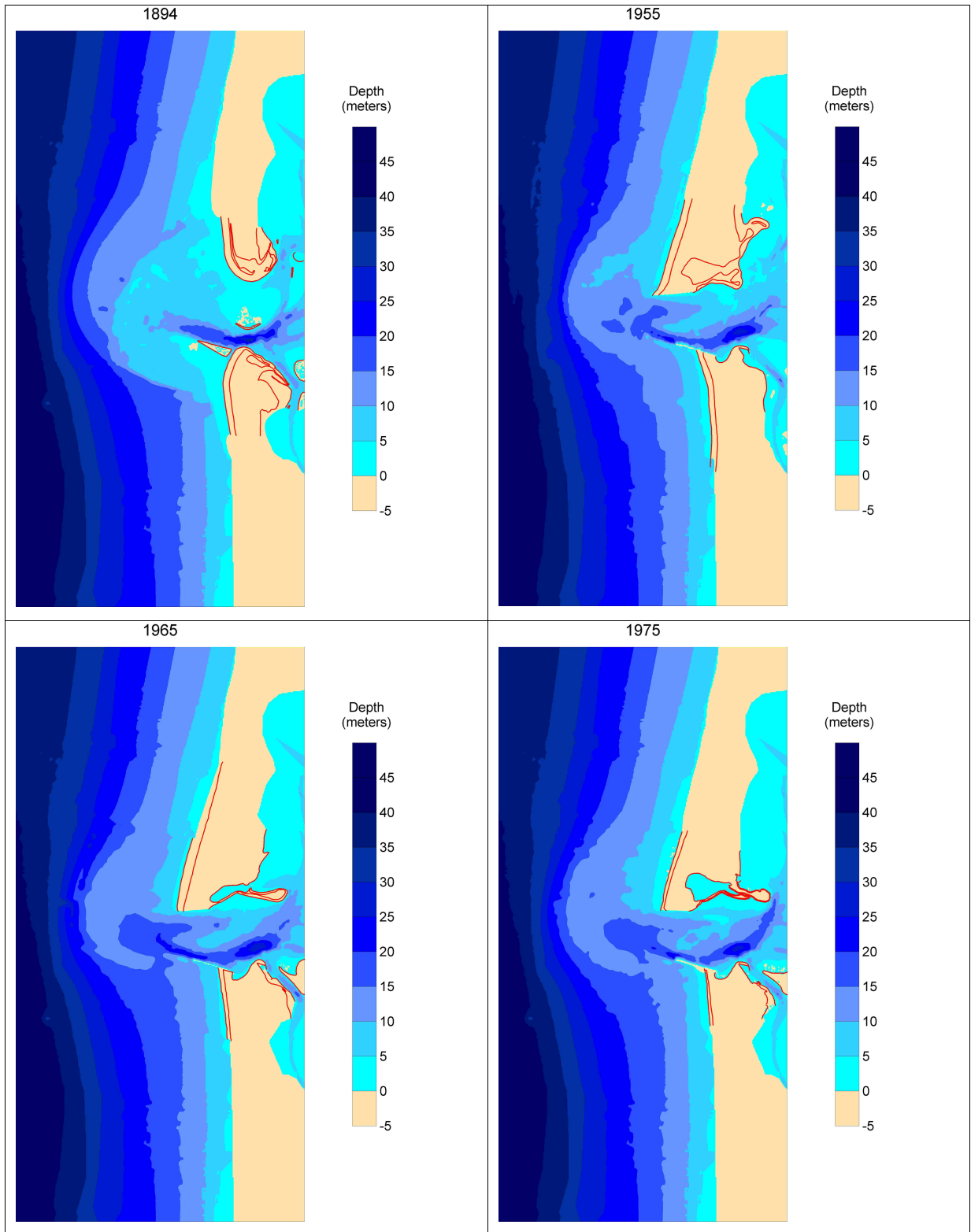


Figure 3-1 Bathymetry grids used for the two-dimensional wave transformation modeling for 1894, 1955, 1965, 1975, 1987, 1993, 1996, and 2002

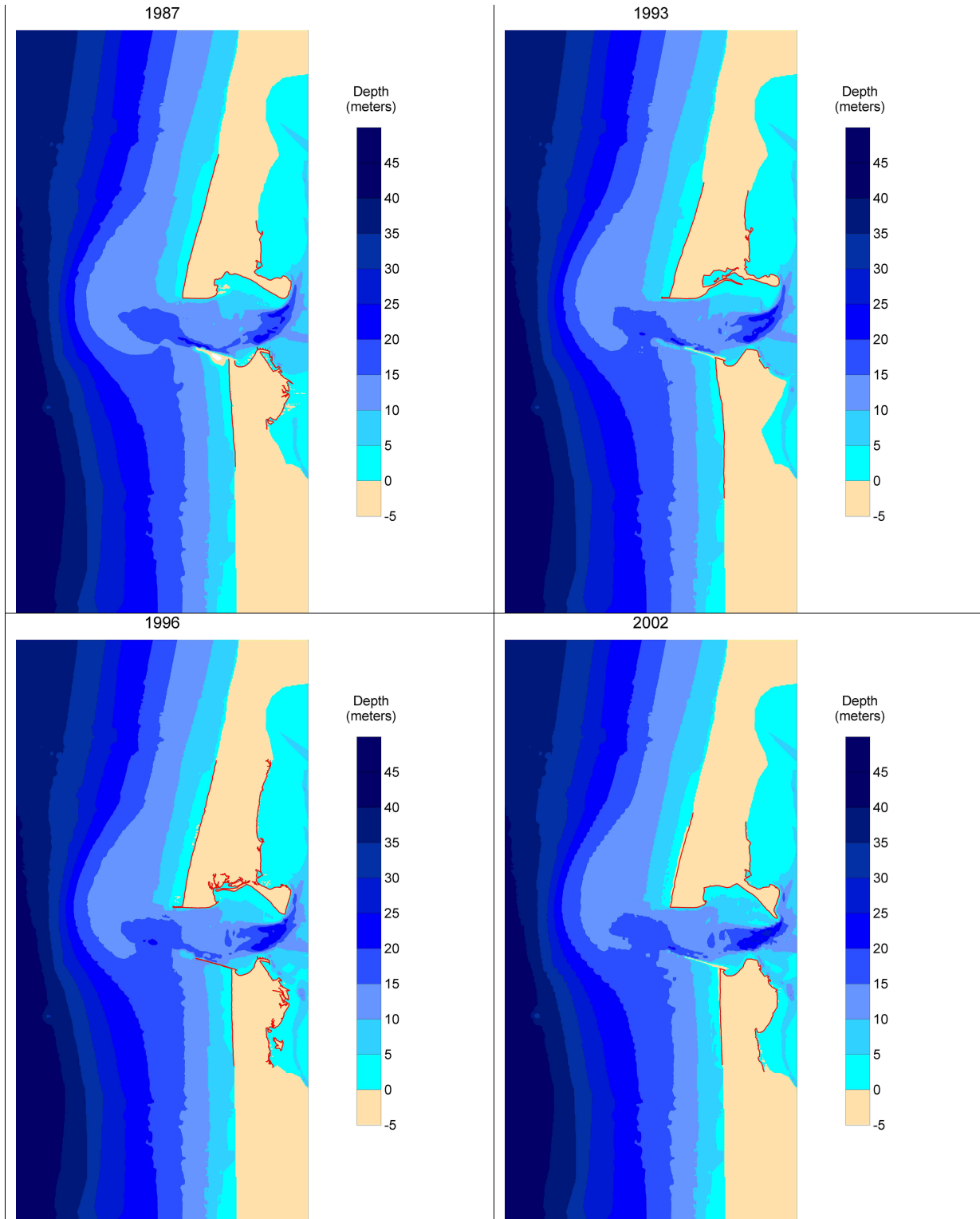


Figure 3-1 Continued

3.3 Selection of Incident Waves for Modeling

Several studies have documented the wave climate of the northeastern Pacific Ocean (e.g., USAED, Seattle 1982; Helmsley and Brooks 1989; Ruggiero et al. (1996), Tillotson and Komar (1997); Allan and Komar (2000a; 2000b; 2001; 2002a; 2002b); and Osborne (2003).

The Grays Harbor, Coastal Data Information Program (CDIP) buoy 03601 has been in operation since 1981, with directional measurements available since 1994. The deep water Naval Oceanographic and Meteorological Device (NOMAD) buoy, operated by NDBC, off the Washington coast (46005) has been in operation since 1976. The offshore boundary for the model grids developed for this study was located at a depth contour consistent with the location of the CDIP buoy. Therefore data from the CDIP buoy were used to develop input boundary conditions for this study.

Significant wave heights (H_s) offshore of Grays Harbor range from less than 1 m to more than 10 m. Peak wave periods (T_p) range from approximately 4 sec up to 24 sec. The combined H_s and T_p distribution for the CDIP buoy 3601 measurements (Figure 3-2) indicates the largest H_s correspond with intermediate wave periods centered between 15 to 18 sec for the Washington coast. A high percentage of waves in the 4 to 6 m range for H_s occur with T_p of 10 to 14 sec. At the CDIP buoy 3601 monthly average H_s varies between 1.2 to 1.7 m in summer months (May-September) and between 2.0 to 2.9 m in winter months (October-April). Monthly average T_p decreases in summer months ranging from 8.1 to 10.4 sec and increases to between 10.6 and 12.9 sec in winter months.

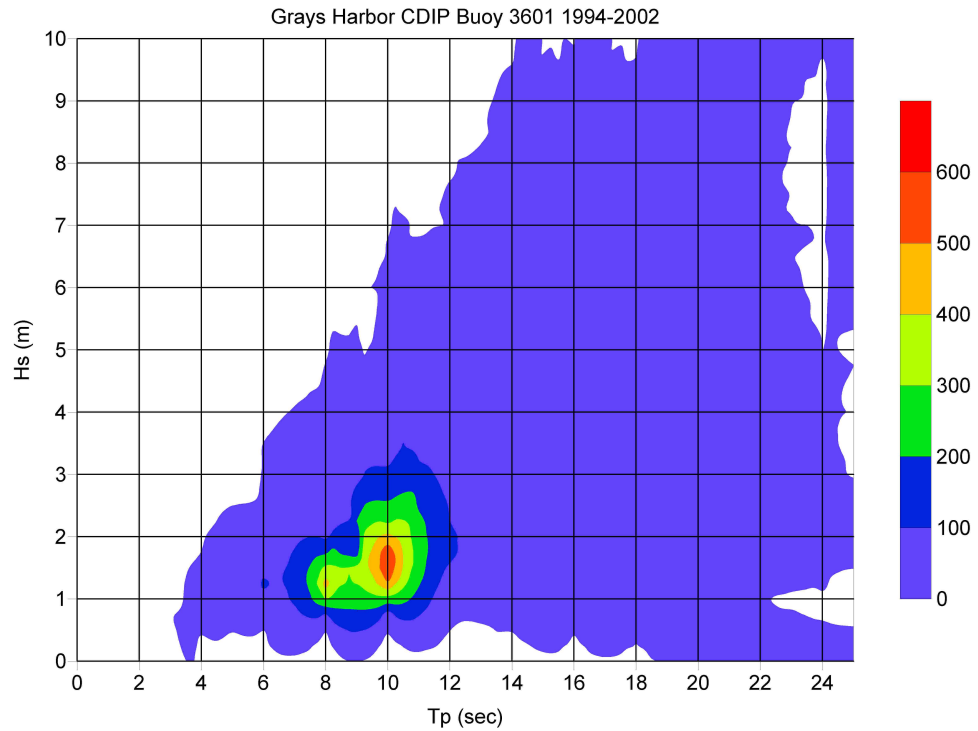


Figure 3-2 Joint distribution of H_s and T_p for measurements at the Grays Harbor CDIP buoy 3601 between January 1994 and December 2002. Color scale represents number of hours per year

Figure 3-3 shows the percent frequency of occurrence for all H_s measured at the CDIP buoy between January 1994 and December 2001 in 11.25 deg bands. The wave rose shows that most waves arriving at Grays Harbor originate from the west and west-northwest.

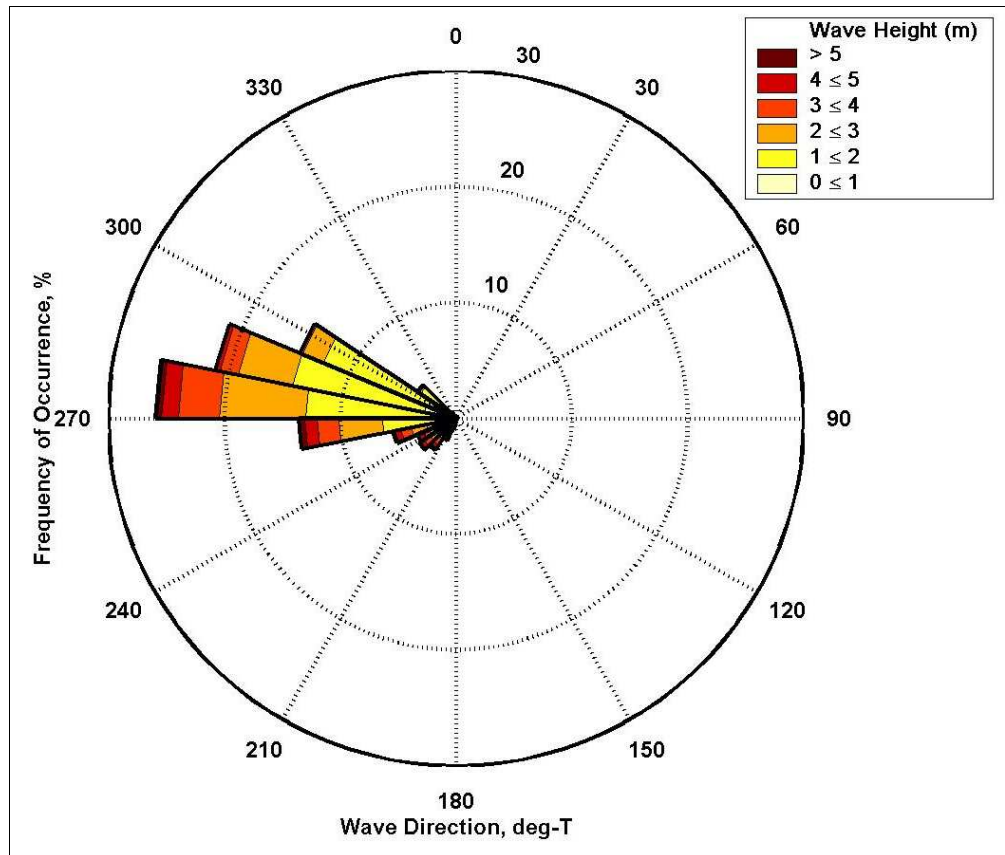


Figure 3-3 Wave rose showing percent frequency of occurrence for all waves in 11.25-deg bands

A previous study conducted by PI Engineering and ERDC-CHL in 2002 performed modeling of wave propagation with STWAVE into the inlet east as far as Whitcomb Flat (e.g. Cialone and Kraus, 2001). The modeling included 60 wave parameter combinations shown Appendix B, as well as wave-current interaction associated with maximum flood currents at mid-tide, slack water at high tide (mhhw), and maximum ebb currents at mid tide or a total of 180 simulations. The depth-averaged ebb and flood current fields were simulated with the Advanced CIRCulation (ADCIRC) model (Luettich et al. 1992). The ADCIRC model for Grays Harbor was calibrated for a bathymetry grid based on hydrographic surveys of the inlet acquired by USAED, Seattle in 1999 and field measurements of currents and water levels in 1999 (Cialone et al. 2002). These data were reviewed for this study to provide an assessment of the effects of tidal currents and incident wave direction on wave heights at Whitcomb Flat.

Two wave conditions were selected for additional modeling and analysis of wave height changes over time at Whitcomb Flat as part of this study. H_s of 4 m, T_p of 12 sec and peak direction of 270 deg were selected to represent a typical storm. H_s of 8 m, T_p of 16 sec and direction of 270 deg were selected

to represent an extreme winter storm event. An extremal peak-over-threshold-analysis for waves with H_s greater than 6.0 m determined from the measurements at the CDIP buoy 3601 between 1981 and 2002 indicates that waves with H_s of 8.0 m have a return period of 2 years (Osborne, 2003).

3.4 Wave Height Changes at Whitcomb Flat (1894 to 2002)

Waves in Grays Harbor entrance are influenced not only by changes in water depth but also by tidal currents in the inlet. Waves propagating from the open ocean into Grays Harbor entrance against the ebb current are steepened (increase in height and reduced length) by the current. Waves propagating with the flood current into the entrance will be reduced in height and increased in length (decrease in steepness). Figures 3-4 and 3-5 show the variations in H_s at and near Whitcomb Flat for the selected waves including the effects of maximum ebb and flood tidal currents and high water slack tide conditions. The analysis indicates that the largest penetration of wave energy to Whitcomb Flat occurs at maximum ebb for the 4 m incident waves and at high tide for the 8 m incident waves. The 8 m waves are reduced in height by depth-controlled breaking at mid-tide, and possibly by oversteepening as a result of wave-current interaction. The smaller 4 m waves are steepened mostly by interaction with the ebb tidal current rather than by water depth. The analysis also determined that the largest waves that penetrate to Whitcomb Flat originate from westerly and west-northwesterly directions.

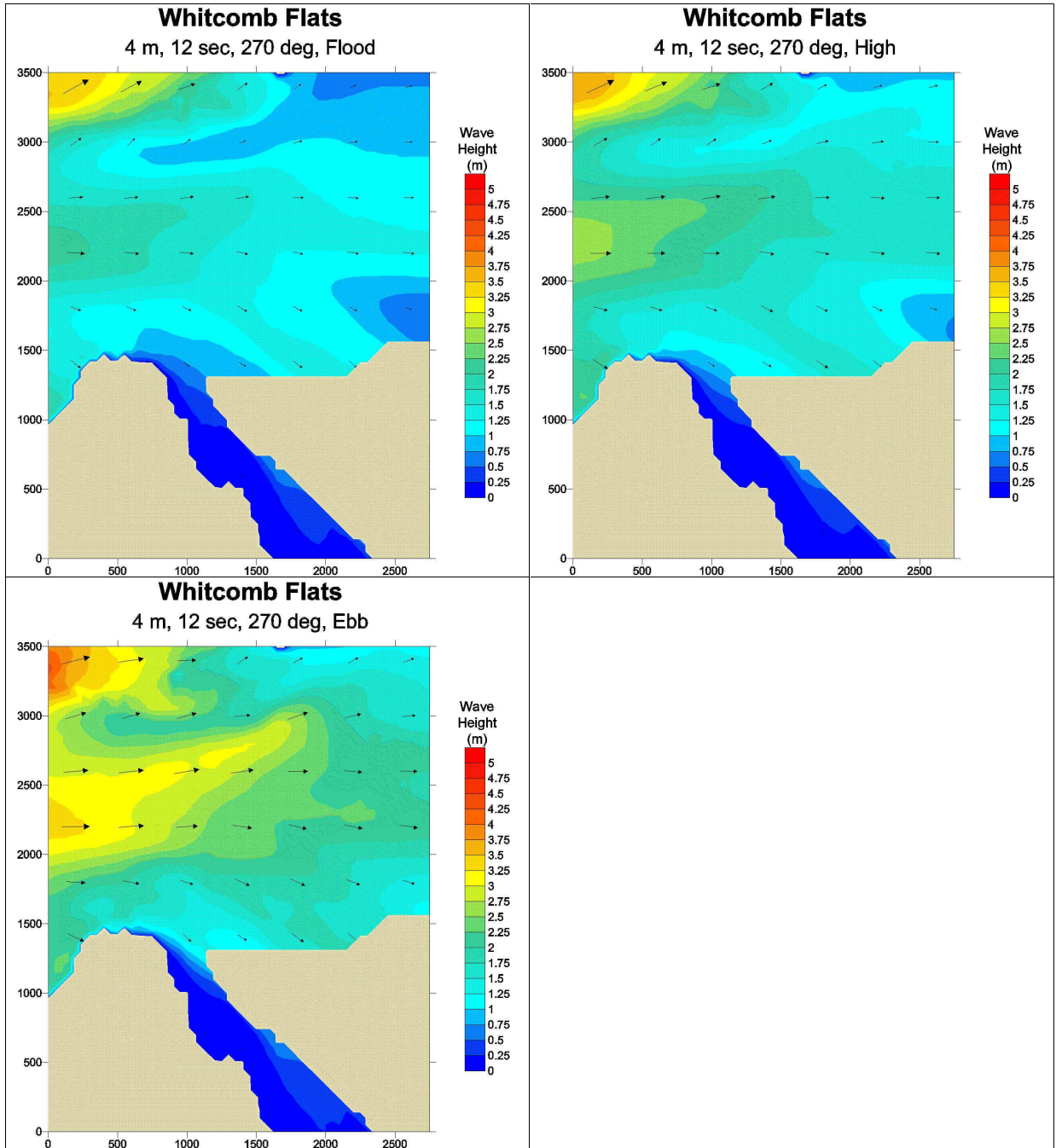


Figure 3-4 Wave height (contours) and wave direction (arrows) as simulated by the STWAVE model for incident H_s of 4 m, T_p of 12 sec, and DIR of 270 deg at maximum flood, mhhw, and maximum ebb

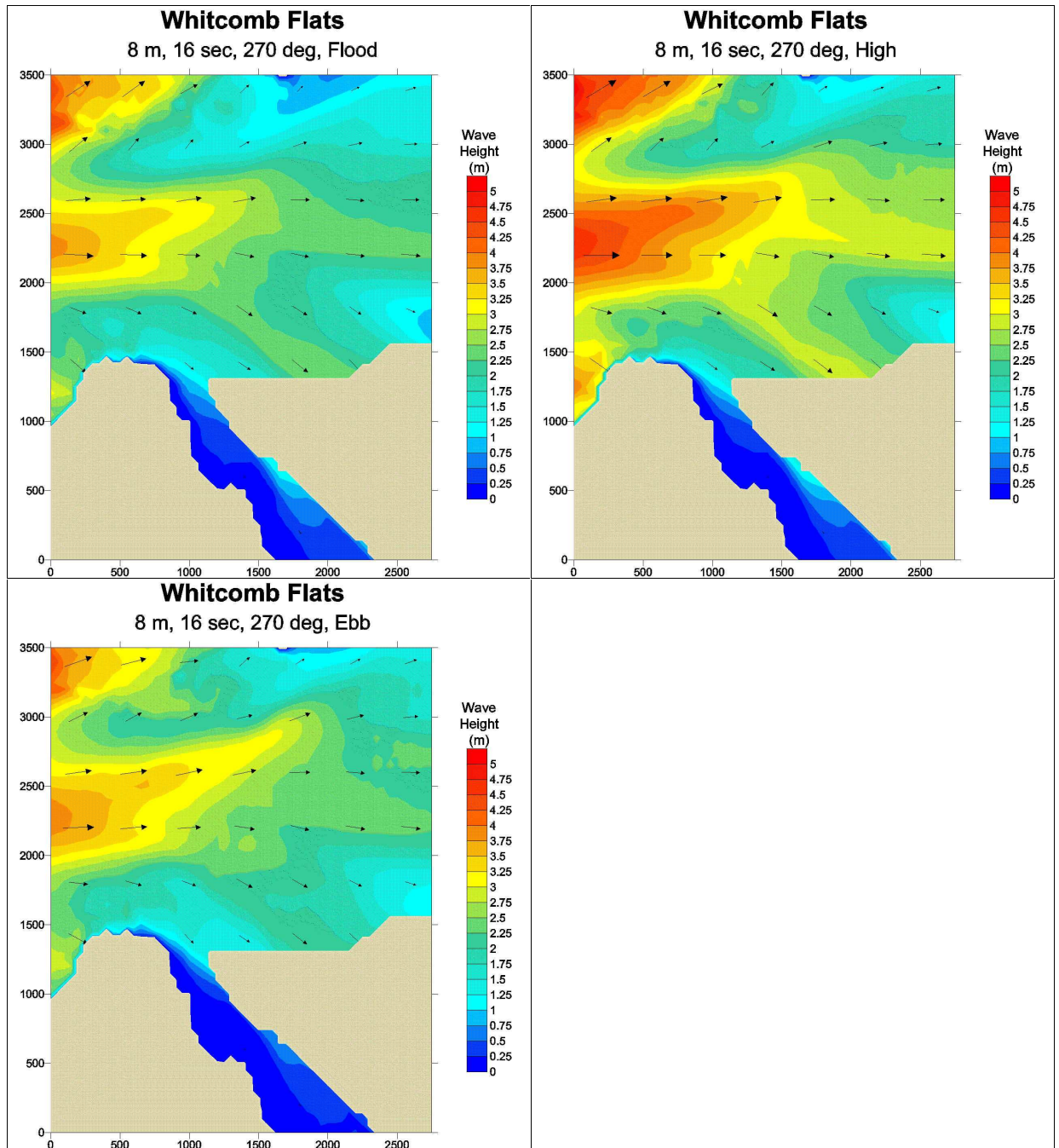


Figure 3-5 Wave height (contours) and wave direction (arrows) as simulated by the STWAVE model for incident H_s of 8 m, T_p of 16 sec, and DIR of 270 deg at maximum flood current at mid tide, mean higher high water, and maximum ebb current at mid tide

Changes in wave height over time at Whitcomb Flat were analyzed by simulating waves for the high water (mhhw) slack condition from 270 deg on the depth grids shown in Figure 3-1. Spatial variations in wave height were evaluated by simulating waves on the bathymetry grids for 1894, 1955, and 2002. Wave heights and bottom elevations were extracted from the model

grid along an east-west transect through the inlet throat from approximately 1500 m seaward of the western end of south jetty to just west of Whitcomb Flat as shown in Figure 3-6. The orientation and position of the transect was chosen such that it could be applied to all three model grids. The cross-shore distances in Figure 3-6 begin at the most seaward point of the transect located near the inlet entrance. Three geographical points of reference are helpful to interpret wave height and depth variations along the transects: the western end of the south jetty is directly south of the 1565 m position on the transect, Point Chehalis is located south of 4720 m, and Damon Point is north of 6160 m. Figure 3-7 shows the depth variations along the transect for 1894, 1955 and 2002.

Figures 3-8 and 3-9 show the patterns of wave height variation along the transect for the 4-m and 8-m incident waves, respectively, for 1894, 1955, and 2002. In 1894, both the 4-m and 8-m incident waves were depth-limited by the time they reached the inlet entrance at the start of the transect. Wave height decreases steadily along the transect except for a slight increase as waves pass over a shoal at approximately 3000 m.

In the 1955 simulation, the 4-m waves gradually increase in height in the inlet entrance to a maximum of approximately 4.8 m and then steadily decrease with distance east along the transect. The increase in wave height is caused by wave shoaling as the depth steadily decreases from the beginning of the transect over a distance of approximately 2000 m. The same pattern is evident for the 8-m waves in 1955. However, the distance of shoaling is much less for the 8-m waves because the larger waves shoal, break, and dissipate energy in deeper water when compared with smaller waves. The wave height decreases gradually along the transect for both the 4-m and 8-m simulations on the 2002 grid. H_s increases at the east end of the transect between 1894 and 1955 and again between 1955 and 2002.

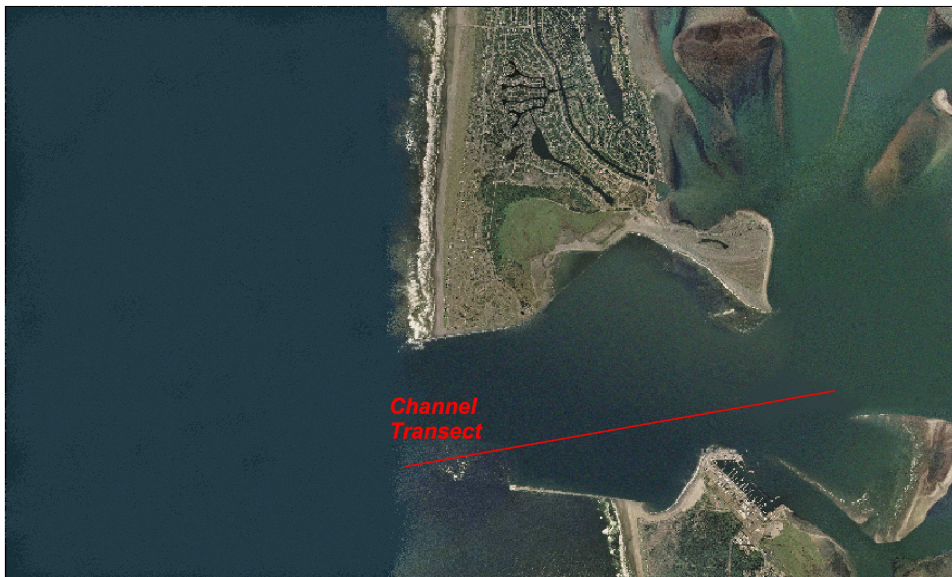


Figure 3-6 Location of transect for analysis of spatial and temporal wave height variation

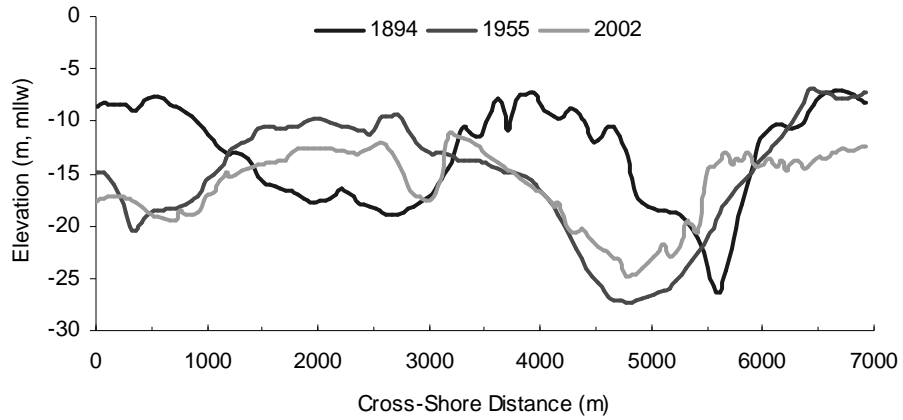


Figure 3-7 Depth variations along a channel transect for 1894, 1955, and 2002 model grids

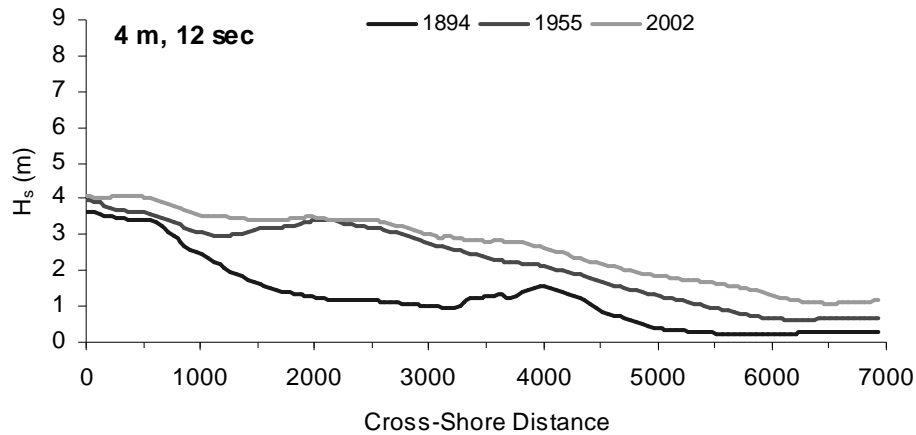


Figure 3-8 Wave height variations along a channel transect for incident waves with H_s of 8 m and T_p of 16 sec

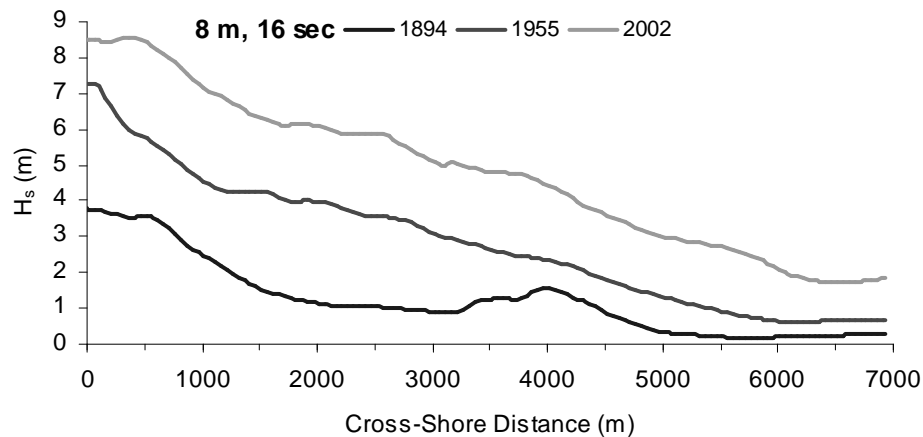


Figure 3-9 Wave height variations along a channel transect for incident waves with H_s of 8 m, and T_p of 16 sec

A more detailed analysis of the temporal variations in wave height at Whitcomb Flat was conducted by simulating waves on the 1955, 1965, 1975, 1987, 1993, 1996, and 2002 bathymetry grids. Figures 3-10 through 3-12 show maps of wave height contours and wave direction for the 4-m and 8-m H_s condition for 1955, 1987 and 2002. In 1955 a portion of the ebb shoal remained on the north side of the inlet resulting in dissipation of wave energy. Waves entering the inlet were focused by refraction on the north side of the inlet near the existing location of Damon Point. At that time, the shoal in the area of Damon Point was an island and the main ebb channel was further north in the inlet throat. Wave heights were generally reduced to less than 1 m near Whitcomb Flat. By 1987, the ebb shoal had continued to erode and move into deeper water and the inlet throat had deepened. Also, by this time, the

subaqueous distal portion of Damon Point was accreting so that the main channel had shifted to the south. These changes in the larger scale geomorphology allowed larger waves to propagate into the inlet and a greater proportion of wave energy to reach Whitcomb Flat. The changes continued between 1987 and 2002. The rate of shoal accretion at Damon Point accelerated forcing the channel south and increasing the size of ocean waves reaching Whitcomb Flat.

Wave heights were extracted from the model grids from a rectangular area adjacent to Whitcomb Flat as shown in Figure 3-13. Figure 3-14 shows the time series of spatially-averaged wave heights for the area shown in Figure 3-13. The time series indicates that both the 4-m and 8-m incident waves have increased in height at Whitcomb Flats since 1955. There has been a much larger increase in the height of the extreme storm waves over this interval because of the increase in depth in the inlet throat and also the shifting of the deepest part of the channel to the south. There is no significant variation in the wave height time series that correlates with either the channel realignment in the late 1970s or the Navigation Improvement Project in the early 1990s. Instead, there is a steady increase in wave height through time which correlates with the larger scale morphological changes that include inlet deepening and throat migration. The above analysis supports the hypothesis that ocean wave processes associated with storm waves are an important mechanism responsible for the migration patterns of Whitcomb Flat.

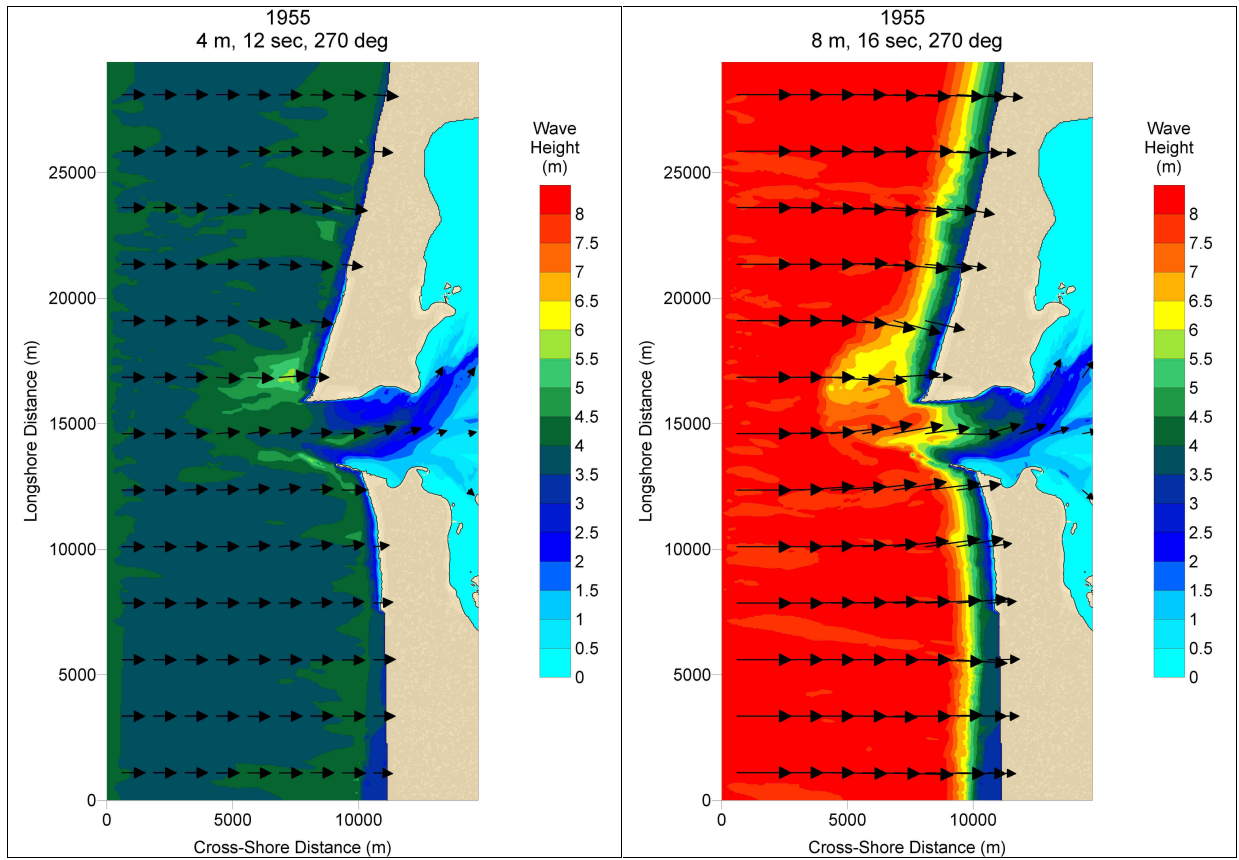


Figure 3-10 Wave height (contours) and wave direction (arrows) as simulated by the STWAVE model for high water slack (right: $H_s = 4$ m, $T_p = 12$ sec, DIR = 270 deg; left: $H_s = 8$ m, $T_p = 16$ sec, DIR = 270 deg) on the 1955 bathymetry

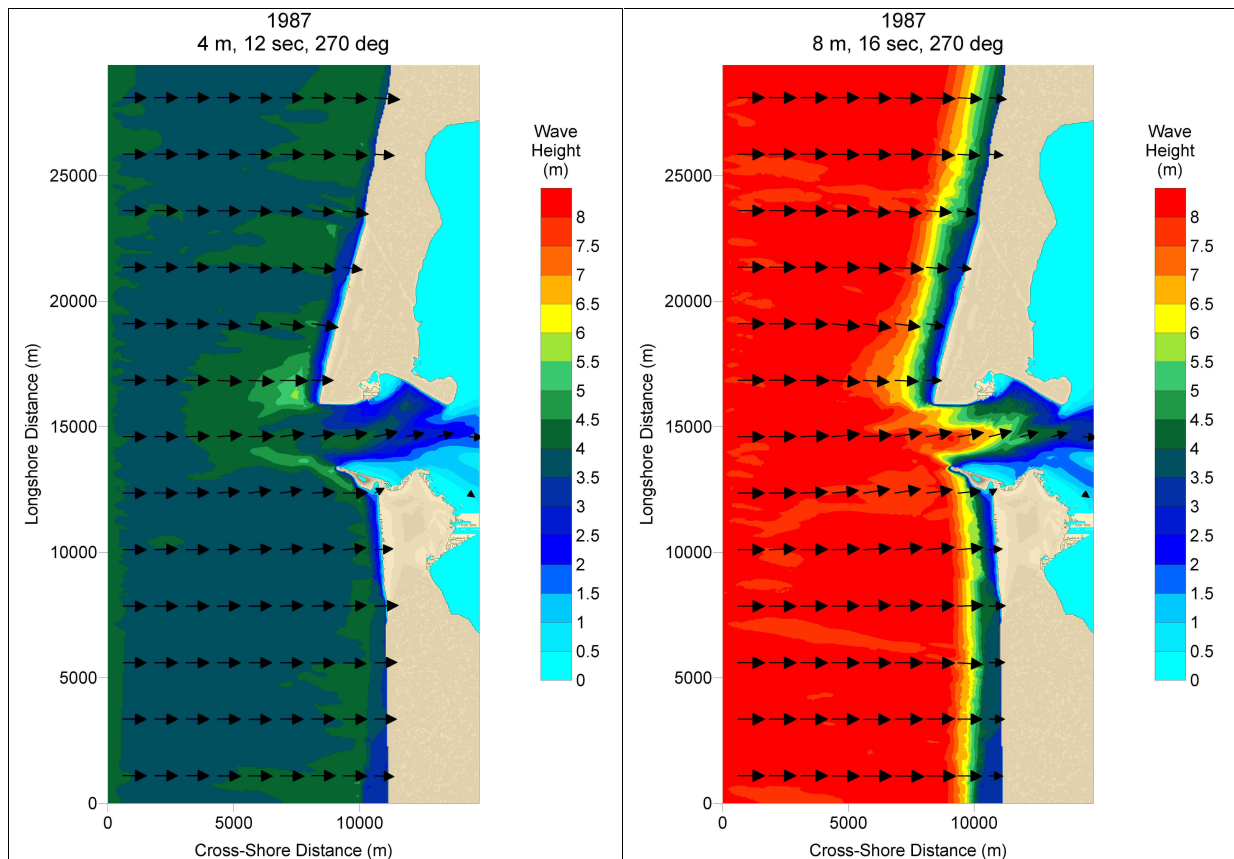


Figure 3-11 Wave height (contours) and wave direction (arrows) as simulated by the STWAVE model for high water slack (left: $H_s = 4$ m, $T_p = 12$ sec, DIR = 270 deg; right: $H_s = 8$ m, $T_p = 16$ sec, DIR = 270 deg) on the 1987 bathymetry

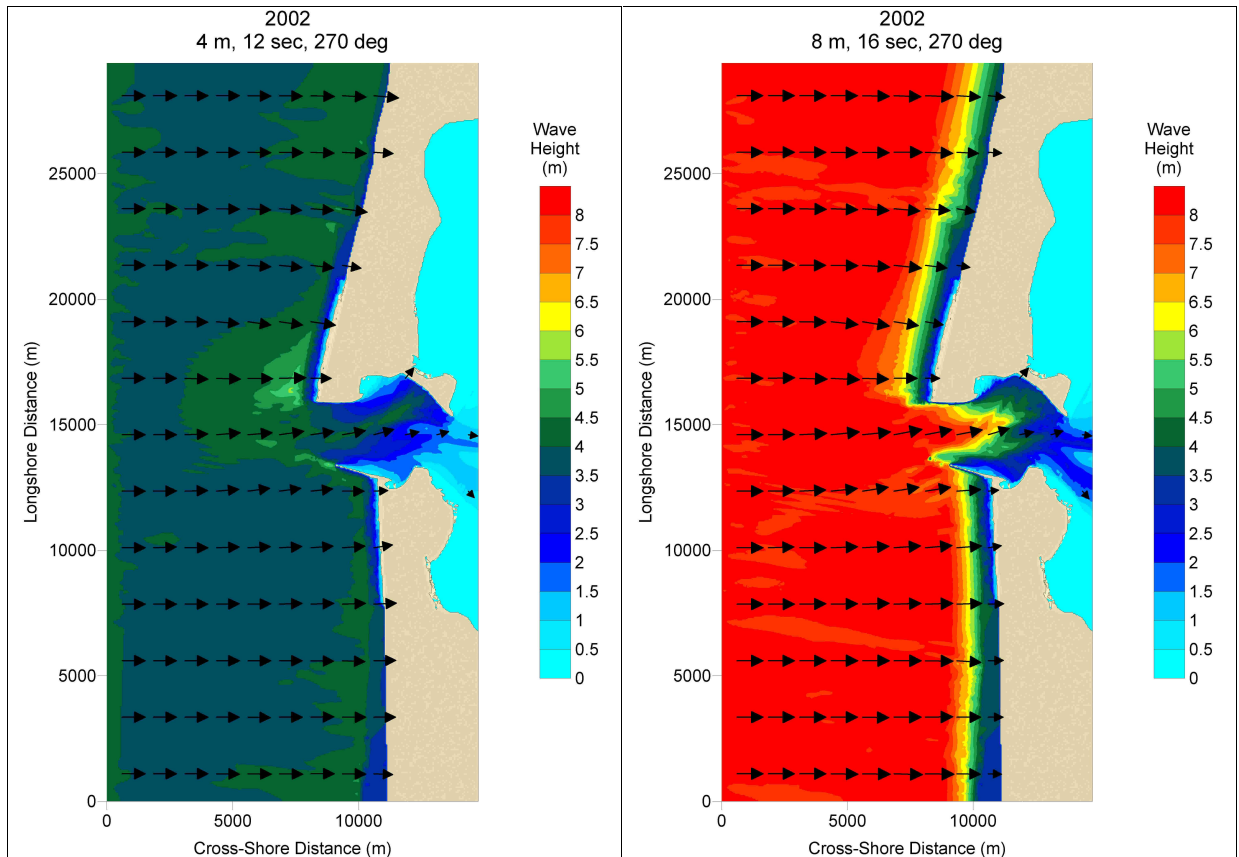


Figure 3-12 Wave height (contours) and wave direction (arrows) as simulated by the STWAVE model for high water slack (left: $H_s = 4$ m, $T_p = 12$ sec, DIR = 270 deg; right: $H_s = 8$ m, $T_p = 16$ sec, DIR = 270 deg) on the 2002 bathymetry

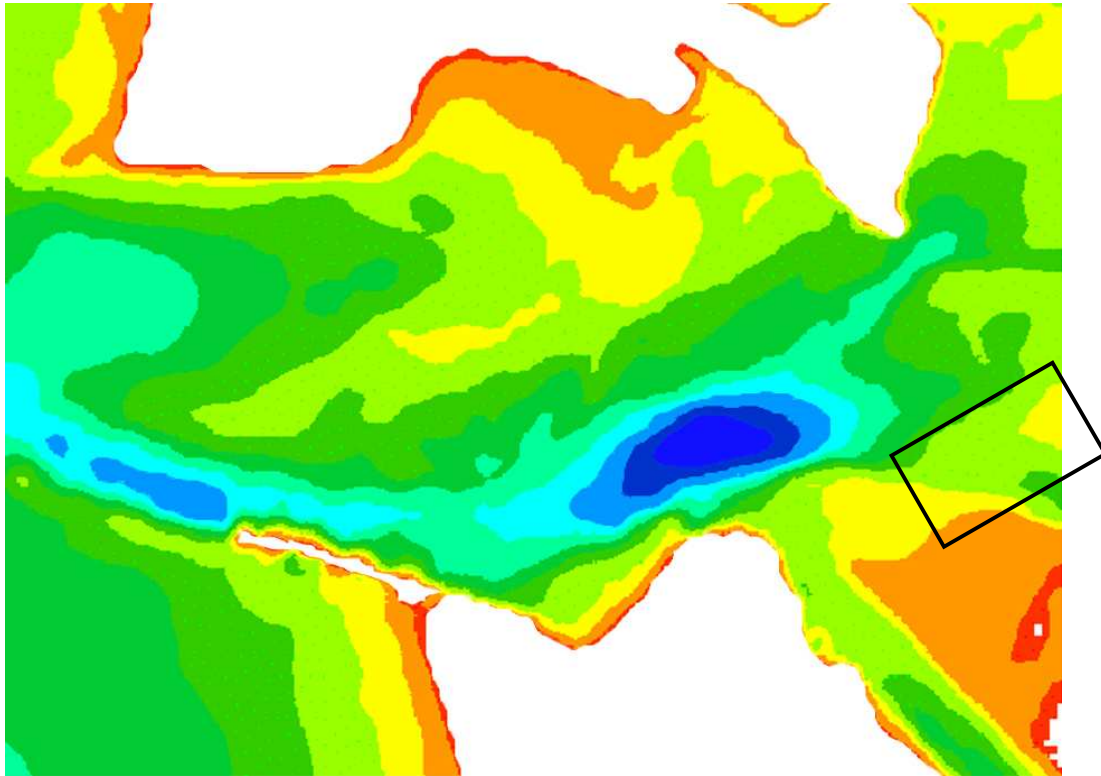


Figure 3-13 Area near Whitcomb Flat for calculating spatially-averaged wave height over time

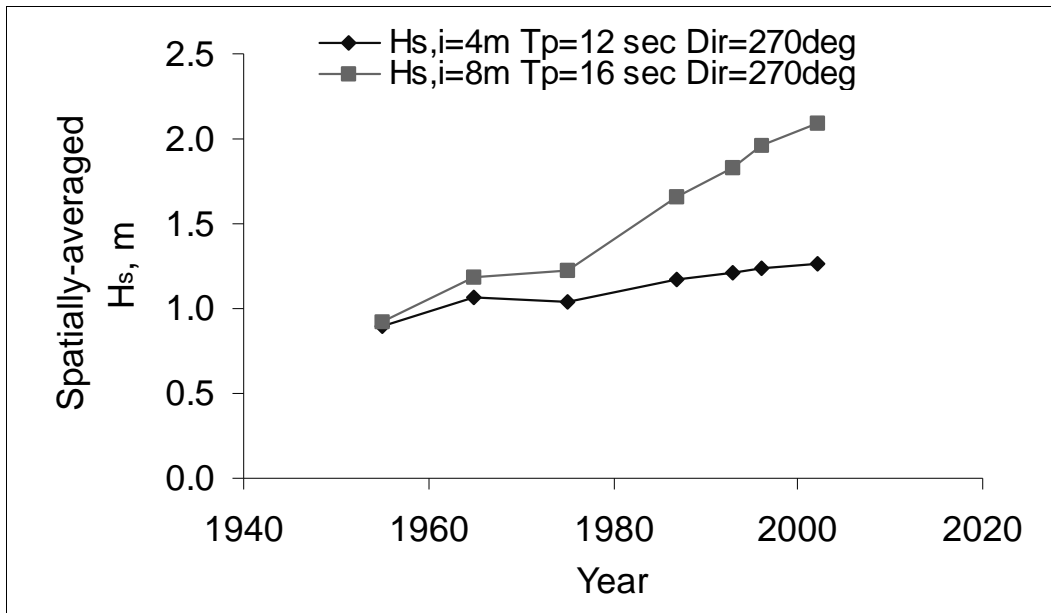


Figure 3-14 Time series of spatially-averaged wave heights at Whitcomb Flat simulated with the STWAVE model for two incident conditions

4. Summary and Discussion

This report provides analysis of the history of the navigation channel, the geomorphology of the inlet throat and the variations in wave height that have occurred in Grays Harbor inlet since jetty construction. The purpose of the analysis is to provide baseline information on physical processes and geomorphology needed to assess potential impacts to Whitcomb Flats by ongoing maintenance of the navigation channel which forms part of the U.S. Army Corps of Engineers (USACE), Grays Harbor and Chehalis River Navigation Project. The information will be of value to assess whether ongoing navigation in the harbor will adversely affect the future formation of spits and shoals within the harbor.

It has long been recognized, that inlet shoals and adjacent shoreline evolution are related and may undergo systematic cycling of sediments (Dean and Walton, 1975; Oertel, 1977). Shoal bypassing (Sexton, 1981; Sexton and Hayes, 1983) for example, in which shoals from the ebb tide shoal periodically migrate to adjacent beaches, is a major process associated with sediment cycling. The mechanisms involved in shoal bypassing and which control the magnitude and frequency of bypassing events are relatively unknown (see Gaudiano and Kana, 2001 for an excellent review). The tidal prism (Kana, 1995), ebb-shoal and bypassing shoal volumes, time-velocity asymmetry of ebb tidal flows (e.g. Hayes, 1980), the interaction of waves with tidal currents (Hayes, 1979), and the littoral sediment supply are all variables that interact to control bypassing events. Bypassing events outside the inlet, in turn, affect the volumes of sediment that may be available for cycling into the harbor by flood-tidal processes and waves that dominate the shorelines adjacent to tidal inlets and the channel margins of the inlet throat. Regional coastal processes outside the inlet that affect sediment supply and sea level are thereby linked with the formation and evolution of flood tidal shoal components such as Whitcomb Flat.

Limited information on the dynamics of sand flats within Grays Harbor estuary exists prior to 1900. However, the most significant recent (last 150 years) geomorphic changes in the inlet were caused by the construction of the jetties between 1898 and 1916 and the major rehabilitation of the jetties in the 1930s and 1940s. Major geomorphic changes occurred in the period 1900 to 1950, and significant adjustments continue to present. The construction of two entrance jetties at Grays Harbor significantly altered the short-term and long-term patterns of sediment cycling in the harbor, while at the same time creating significant improvements for navigation.

Jetty construction and subsequent rehabilitation in the 1930s and 1940s resulted in significant changes to the inlet tidal hydraulics and distribution of major morphological features. When functioning correctly, the jetties cause constriction of the ebb dominant tidal currents in the inlet throat, creating a jet-like flow at the entrance that extends several miles seaward of the entrance. The result has been scour of the seabed in the entrance, offshore transport of sediment, and shifting of the ebb shoal into deeper water. The jetties also serve to block a significant amount of littoral sediment transport, both north and south of the entrance, reducing inlet

sedimentation associated with flood tidal processes and waves. In contrast, the periods of jetty deterioration between construction and rehabilitation (1916 to 1940 and 19405 to 1965) have promoted the growth and development of spits along the margins of the inlet throat and deposition on the flood shoals to the east of the inlet throat. Continued development of the spits and shoals on the south side of the inlet has been restricted since the 1950s by construction of the rock armor protection and groins at Point Chehalis.

More recently, the rehabilitation of the north jetty in 1975 had a relatively minor impact on inlet throat erosion and spit development in the inlet. This is because the 1975 rehabilitation did not affect the length or sand blocking function of the jetty. In recent years, significant sand bypassing at North Jetty has lead to accretion of the spits and shoals on the north side of the inlet entrance. Damon Point, a large sand spit attached to the eastern end of the north jetty, has been accumulating sand since the 1960s at a rate of approximately 450,000-600,000 cu yd/year. Similarly, sand accumulation has also been occurring at Sand Island Shoal on the north side of the main channel north of Whitcomb Flat. This accumulation led the USAED, Seattle to realign the navigation channel from Sand Island Reach to South Reach in 1978. Dredging volumes at the South Reach have decreased significantly in the past decade relative to previous decades despite the widening and deepening project in 1990-91. The amount of sediment dredged at the South Reach has been relatively stable over the latter part of the last decade since the Navigation Improvement Project. The recent reduction in dredging in this area correlates with the inlet throat erosion that has been ongoing in this area for the last several decades. Approximately 900,000 cy/yr of sediment on average has been dredged from the combined outer reaches of the navigation channel (including the Bar Channel, Entrance and Point Chehalis Reaches, South Reach, and Crossover Reach) over the past decade and a half. According to the sediment budget analysis by Byrnes and Baker (2003), the volume of sediment dredged is approximately 16 percent of the gross sediment volume flux in the inlet throat area and approximately 39 percent of the net erosion volume for the area as determined by bathymetry change between 1987 and 2002. Analysis of cross-sections of the main ebb channel to the north of Whitcomb Flat extracted from historical bathymetry surfaces suggests that the widening and deepening project in 1990-91 and ongoing maintenance of the channel cross-section by dredging alone cannot account for the observed changes that have occurred in the geometry of the main ebb channel in the area adjacent to Whitcomb Flat over the last 15 years. Bathymetry change and sediment budget analysis indicate that the annualize gross and net volume fluxes (that include dredging) do not differ significantly for the interval 1955 to 1987 relative to the interval 1987 to 2002. The depth changes in the South Reach area appear to be linked to the larger scale trends in inlet geomorphology that are occurring as well as to local scale changes that include dredging activity.

Sand Island shoal and Whitcomb Flat, form the remains of the flood shoal complex that was present prior to jetty construction. In contrast with Damon Spit and Sand Island shoal on the north side of the inlet, geomorphic change at Whitcomb Flat has been dominated by eastward migration of the sand flat. The migration of the main

ebb channel is correlated with the southeastward growth of Damon Point spit and with the associated hydraulic changes in the main ebb channel. The rate of accretion of sediment on Damon Point has increased and the rate of eastward migration of Whitcomb Flat has increased in the last 10 to 20 years. The southeastward growth of Damon Point causes the hydraulic resistance in the inlet throat to increase and in turn constricts the tidal discharge through the inlet throat resulting in local acceleration of the tidal currents. The accretion also forces the main body of the current to the south side of the inlet. Scour, dredging, and southward migration of the channel have all contributed to the increased in depth in the inlet throat, particularly toward the south side of the inlet. The increase in depth allows penetration of larger ocean waves to the south side of the inlet and has also lead to focusing of ocean wave energy on the south side of the inlet throat. Consequently, a much larger increase in the height of the extreme storm waves reaching Whitcomb Flat has occurred because of the increase in depth in the inlet throat and the shifting of the deepest part of the channel to the south over the last two to three decades. Analysis of wave height variation over time at Whitcomb Flat indicates that no significant variation in the prevailing wave height trends is associated with either the channel realignment in the late 1970s or the Navigation Improvement Project in the early 1990s. Instead, there is a steady increase in wave height through time which correlates with the morphological changes that are occurring on a broader scale than the dredged areas of the navigation channel.

The eastward migration of Whitcomb Flat appears to be caused by a combination of factors that may include: wave-induced washover processes and erosion by storm waves; tidal transport; a reduction in sediment supply caused by armoring of the shoreline on the south side of the inlet at Point Chehalis in the 1950s, and perhaps to a lesser extent aeolian transport by prevailing westerly winds. Relocation of the navigation channel from Sand Island Reach to South Reach in the late 1970s, maintenance dredging at South Reach, and the widening and deepening project in the 1990s have also contributed to the overall increase in depth locally that has allowed larger waves to reach Whitcomb Flat. Ebb-dominant tidal currents in the main ebb tidal channel and the Ocosta Channel immediately adjacent to Whitcomb Flat have caused the growth of spits westward off each end of the long axis of Whitcomb Flat. Wave and current impacts at Whitcomb Flat have been exacerbated mainly by large-scale southward migration of the inlet throat particularly between Damon Point and Point Chehalis which have resulted in increased depth on the south side of the inlet throat. Although channel relocation, dredging, and deepening projects have also contributed to deepening and likely also to enhancement of tidal flow in the South Reach area, the channel position and side slope position between 20 and 40 ft have been relatively stable in the last decade. In contrast, the rate of eastward migration of the sub-aerial and inter-tidal portion of Whitcomb Flat has increased significantly in the past decade. Eastward migration of the sub-aerial and inter-tidal portion of the flat is most likely associated with sediment transport induced by waves and wave overtopping processes rather than tidal flows because tidal flows are primarily ebb dominated in this area, also tidal current velocities decrease rapidly over the tidal flats. It is also likely that the increase in the rate of eastward migration of Whitcomb

Flat is non-linearly related to local increases in wave height through the sediment transport. Eastward migration of the crest of the sand flat is expected to increase as the incidence of overtopping increases and as the percentage of a tidal cycle increases during which wave overtopping occurs. Overtopping events will correlate with periods of super elevation of the water surface that are a direct function of offshore incident wave height. Unfortunately, relatively little information exists with which to evaluate overtopping frequency and the relative roles of wave and tide transport over the flat.

The analysis provides some limited insight regarding options and alternatives that may be suitable for mitigating the migration and erosion of Whitcomb Flat should that prove to be desirable. Alternatives include direct structural and non-structural intervention (soft solution) in the sediment transport processes that cause sand flat erosion and migration as well indirect measures that may influence the processes favorably.

Southward migration of the main ebb tidal channel appears to be closely correlated with accretion of sediment on the south side of Damon Point. Therefore, an indirect approach at addressing the migration and erosion at Whitcomb Flat might be to reduce the volume of sediment reaching Damon Point by reducing the sediment volume that enters the inlet at the north jetty (e.g Kraus and Arden, 2003). Such an approach could potentially be expected to contribute to reducing erosion and eastward migration of Whitcomb Flat in the long term (one to two decades). A more direct non-structural approach would be to consider nourishment of Whitcomb Flat to reduce overtopping storm waves and swell. Design of any solution should be developed from the results of a focused monitoring program (minimum 5 years) and a comprehensive analysis of alternatives. Monitoring should include collection of data on dredging and disposal practices in the inlet, high resolution aerial photographs, detailed and high resolution surveys of sub-aerial, inter-tidal and sub-tidal sand flat morphology, and measurements of forcing mechanisms local to Whitcomb Flat including wave heights, water levels and sediment transport rates.

5. References

- Allan, J. C., and Komar, P. D. (2000a). "Spatial and temporal variations in wave climate of the North Pacific," Report to the Oregon Department of Land Conservation and Development, 46 p.
- Allan, J. C., and Komar, P. D. (2000b). "Long-term and climate-related increases in storm wave height in the North Pacific," *EOS Transactions* 47, American Geophysical Union, 561-567.
- Allan, J. C., and Komar, P. D. (2001). "Wave climate change and coastal erosion in the US Pacific Northwest," *Proceedings of the 4th Conference on Ocean Wave Measurement and Analysis, WAVES 2001*, San Francisco, CA, ASCE, pp. 680-690.
- Allan, J. C. and Komar, P. D. (2002a). "The wave climate of the eastern North Pacific: Long-term trends and an El Niño/La Niña dependence," Southwest Washington Coastal Erosion Workshop 2000, G. Gelfenbaum, and G. M. Kaminsky (eds.), Open-file-report 02-229.
- Allan, J.C. and Komar, P.D. (2002b). "Extreme storms on the Pacific Northwest Coast during the 1997-98 El Niño and 1998-99 La Niña." *Journal of Coastal Research*, 18(1), 175-193.
- Black, W.M. (1916). Letter to the Secretary of War, In Letter from Secretary of War transmitted to Congress, December 12, 1916.
- Board of Engineers for Rivers and Harbors. (1934). "Report of the Board of Engineers for Rivers and Harbors to the Chief of Engineers, United States Army, Subject: Grays Harbor, Washington, June 26, 1934," in letter transmitted to Committee on Rivers and Harbors, 74th Congress, July 17, 1934.
- Buijsman, M.C., Kaminsky, G.M., and Gelfenbaum, G. (2003). Shoreline change associated with jetty construction, deterioration, and rehabilitation at Grays Harbor, Washington., *Shore and Beach*, 71(1), 15-22.
- Burch, T.L. and Sherwood, C.R. (1992). "Historical bathymetric changes near the entrance to Grays Harbor, Washington," Batelle/Marine Sciences Laboratory Sequim, Washington.
- Byrnes, M.R. and Baker, J.L. (2003). Inlet and nearshore morphodynamics. In North Jetty. Chapter 3 in N.C. Kraus, and H.T. Arden, (eds.) North Jetty Study, Grays Harbor, Washington. Volume I: Main Text. ERDC-CHL-TR-03-X.
- Byrnes, M.R., Baker, J.L., and Krause, N.C. (2003). "Coastal sediment budget for Grays Harbor, Washington." *Proceedings of Coastal Sediments 2003*, Clearwater Beach, Florida.
- Cialone, M.A. and Kraus, N.C. (2001). "Engineering study of inlet entrance hydrodynamics: Grays Harbor, Washington, USA." *Proceedings 4th Coastal Dynamics Conference*, ASCE, 413-422.
- Cialone, M.A., Millitello, A., Brown, M.E., and Kraus, N.C. (2002). Coupling of wave and circulation numerical models at Grays Harbor entrance, Washington, USA.. *Proceedings 28th ICCE 2002*, World Scientific, 1279-1291, in press.
- Committee on Tidal Hydraulics (1967). Grays Harbor, Washington. U.S. Army Corps of Engineers, ARMYMRC Vicksburg. Mississippi, USA.
- Dean, R.G. and Walton, T.L. (1975). Sediment transport processes in the vicinity of inlets with special reference to sand trapping. In: Cronin, L.E. (Ed.) Estuarine Research Conference, Vol. 2, New York: Academic, pp. 129-149.

References

- Gaudio, D.J. and Kana, T.W. (2001). Shoal bypassing in mixed energy inlets: geomorphic variables and empirical predictions for nine South Carolina inlets. *Journal of Coastal Research*, 17 (2): 280-291.
- Hayes, M.O. (1979). Barrier island morphology as a function of tidal and wave regime. In: Leatherman, S. (ed.), *Barrier Islands*, New York: Academic, pp. 1-26.
- Hayes, M.O. (1980). General morphology and sediment patterns in tidal inlets. *Sedimentary Geology*. 26, pp. 139-156.
- Helmsley, J. M., and Brooks, R. M. (1989). "Waves for coastal design in the United States," *Journal of Coastal Research* 5, 639-663.
- Kaminsky, G.M., Ruggiero, P., McCandless, D., Lindstrum, E., McInnis, J., and Daniels, R. (1999). "Road wash-outs and shoreline change at Damon Point, Washington", Report to the Washington State Parks and Recreation Commission, Olympia, Washington.
- Kana, T.W. (1995). Signatures of coastal change at mesoscales. *Coastal Dynamics '95, Proceedings of the International Conference on Coastal Research in Terms of Large Scale Experiments*. ASCE, NY, pp. 987-997.
- Kraus, N.C. and Arden, H.T. (2003). (eds.) North Jetty Study, Grays Harbor, Washington. Volume I: Main Text. ERDC-CHL-TR-03-X. Draft Technical Report.
- Luetlich, R. A., Westerink, J. J., and Scheffner, N. W. (1992). ADCIRC: An advanced three-dimensional circulation model for shelves, coasts, and estuaries; Report 1, Theory and methodology of ADCIRC-2DDI and ADCIRC-3DL, Technical Report DRP-92-6, U.S. Army Engineer Waterways Experiment Station, Vicksburg, MS.
- Oertel, G.F. (1977). Geomorphic cycles in ebb deltas and related patterns of shore erosion and accretion. *Journal of Sedimentary Petrology*. 47: 1121-1131.
- Osborne, P.D. (2003). "Oceanographic setting: field measurements and analysis". Chapter 4, in N.C. Kraus, and H.T. Arden, (eds.) North Jetty Study, Grays Harbor, Washington. Volume I: Main Text. ERDC-CHL-TR-03-X.
- Osborne, P.D. and Arden, H.T. (2003). "Grays Harbor and Chehalis River Navigation Project." Chapter 2, in N.C. Kraus, and H.T. Arden, (eds.) North Jetty Study, Grays Harbor, Washington. Volume I: Main Text. ERDC-CHL-TR-03-X.
- Osborne, P.D., Wamsley, T.V., and Arden, H.T. (2003a) "South Jetty sediment processes study, Grays Harbor, Washington: Evaluation of engineering structures and maintenance measures ERDC-CHL-TR-0304." U.S. Army Corps of Engineers, Engineer Research and Redevelopment Charter.
- Osborne, P.D., Davies, M.H., and Cialone, M.A. (2003b). "Sediment transport paths at Grays Harbor." *Proceedings of Coastal Sediments 2003*. Clearwater Beach, Florida.
- Osborne, P.D., Hericks, D.B., Kraus, N.C., and Parry, R.M. (2003c). "Wide-area measurements of sediment transport at a large inlet; Grays Harbor, WA." *Proceedings of 28th International Conference on Coastal Engineering*, Cardiff, Wales, ASCE, pp.
- Permanent International Association of Navigation Congresses (1987) "Guidelines for the design and construction of flexible revetments incorporating geotextiles for inland waterways," Working Group 4 of the Permanent Technical Committee, Brussels.

- Peterson, C.D., and Phipps J.B. (1992). "Holocene sedimentary framework of Grays Harbor basin, Washington, USA," *SEPM Special Publication No. 48*, Society for Sedimentary Geology, 273-285.
- Peterson, C., Scheidegger, K., and Komar, P. (1984). "Sediment composition and hydrography in six high-gradient estuaries of the northwestern United States," *Journal of Sedimentary Petrology*, 54(1), 86-97.
- Phipps, J.B. and Smith, J.M. (1978). "Coastal Accretion and Erosion in Southwest Washington", Washington Department of Ecology Report No. WA/DOE/CZ-78-12, 79 pp. + appendices.
- Resio, D. T. (1987). "Shallow-water waves, Report I: Theory," *Journal of Waterway, Port, Coastal, and Ocean Engineering*, 113(3), 264-281.
- Ruggiero, P., Kaminsky, G. M., Komar, P. D., and McDougal, W. G. (2001). "Extreme waves and coastal erosion in the Pacific Northwest," *3rd International Symposium on Ocean Wave Measurement and Analysis*, 947-961.
- Scheidegger K.F., and Phipps, J.B. (1976). "Dispersal patterns of sands in Grays Harbor estuary, Washington," *Journal of Sedimentary Petrology*, 46(1), 163-166.
- Sexton, W.J. 1981. Natural bar bypassing of sand at Captain Sams Inlet, South Carolina. Unpublished M.Sc. thesis, Dept of Geology, Univ. South Carolina, 148p.
- Sexton, W.J. and Hayes, M.O. 1983. Natural bar bypassing of sand at tidal inlet. *Proceedings 18th Coastal Engineering Conference*, ASCE, NY, pp. 1479-1495.
- Smith, J.M., Sherlock, A. R., and Resio, D.T. 2001. STWAVE: Steady-state spectral wave Model User's Manual for STWAVE Version 3.0. CE-ERDC/CHL IR-01-1, U.S. Army Engineer Research and Development Center, Coastal and Hydraulics Laboratory, Vicksburg, MS.
- Sorensen, R.M. (1997). "Prediction of vessel-generated waves with reference to vessels common to the upper Mississippi River System." Interim Report for the Upper Mississippi River – Illinois Waterway System Navigation Study, TA7 W3499 R5U7 ENV Report 4, 29p.
- Tillotson, K. J., and Komar, P. D. (1997). "The wave climate of the Pacific Northwest (Oregon and Washington): A comparison of data sources," *Journal of Coastal Research* 13, 440-452.
- U.S. Army Engineer District, Seattle (1965). "South jetty rehabilitation." Grays Harbor and Chehalis River Washington General Design Memorandum, U.S. Army Engineer District, Seattle, Seattle, WA.
- U.S. Army Engineer District, Seattle. (1973). "North Jetty Rehabilitation, Grays Harbor and Chehalis River and Hoquiam River, Washington." Department of the Army, Seattle District, Corps of Engineers, September 1973, 34p.
- U.S. Army Engineer District, Seattle. (1974). "Design Memorandum: North Jetty Rehabilitation." Department of the Army, Seattle District, Corps of Engineers, August 1974, 16p.
- U.S. Army Engineer District, Seattle. (1982). "Appendix D – Engineering design and cost estimates." In: Interim Feasibility Report and Final EIS, Grays Harbor, Chehalis and Hoquiam Rivers, Washington Channel Improvement for Navigation, Seattle, WA, 800 p.
- U.S. Army Engineer District, Seattle. (1989). "Grays Harbor, Washington, Navigation Improvement Project", General Design Memorandum and Environmental Impact Statement Supplement, Appendix B- Design Analysis, U.S. Army Corps of Engineers, Seattle District.

References

- U.S. Army Engineer District, Seattle (2001). "Analysis of future dredging requirements: Entrance Channel, Point Chehalis Reach, South Reach, and Crossover Channel. Stations 280+89 to 862+49, Grays Harbor, Washington, Navigation Project". USAED, Seattle, Engineering and Construction Division, 17 p.
- Washington State Department of Ecology. (1977). "Maintenance dredging and the environment of Grays Harbor Washington summary report," Prepared for U.S. Army Engineer District, Seattle, Contract No. DACW67-74-C-0086, 102 p.
- Weggel, J.R. and Sorensen, R.M. (1984). "Ship wave prediction for port and channel design." *Proceedings of the Ports '86 Conference*, Oakland, CA, 19-21 May 1986. Paul H. Sorensen, ed., ASCE, NY, 797-814.



APPENDIX A.

Bathymetric Surfaces for Grays Harbor Main Channel 1956 to 2002

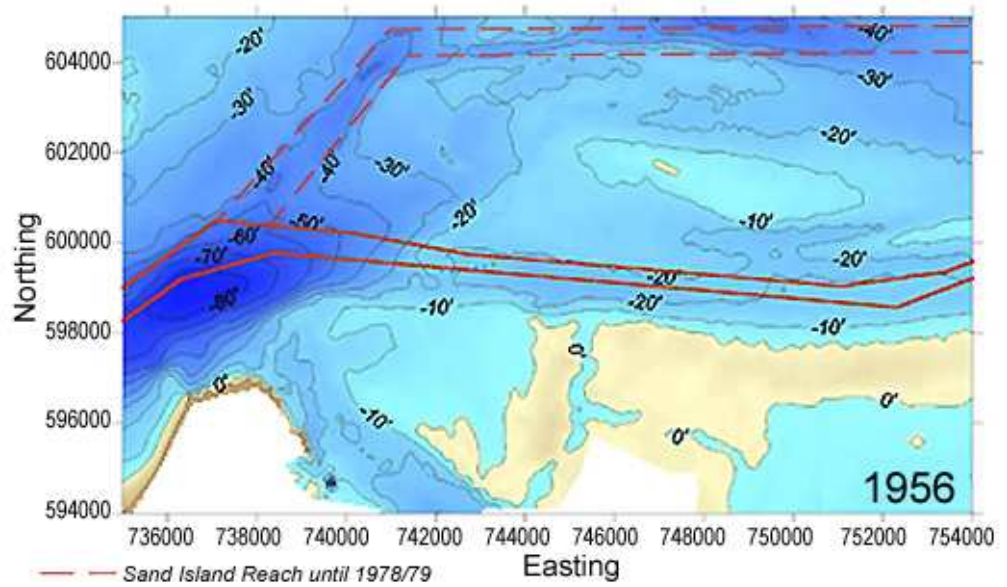


Figure A-1 Bathymetric surface for Grays Harbor main channel in 1956. Depths are feet, mllw.

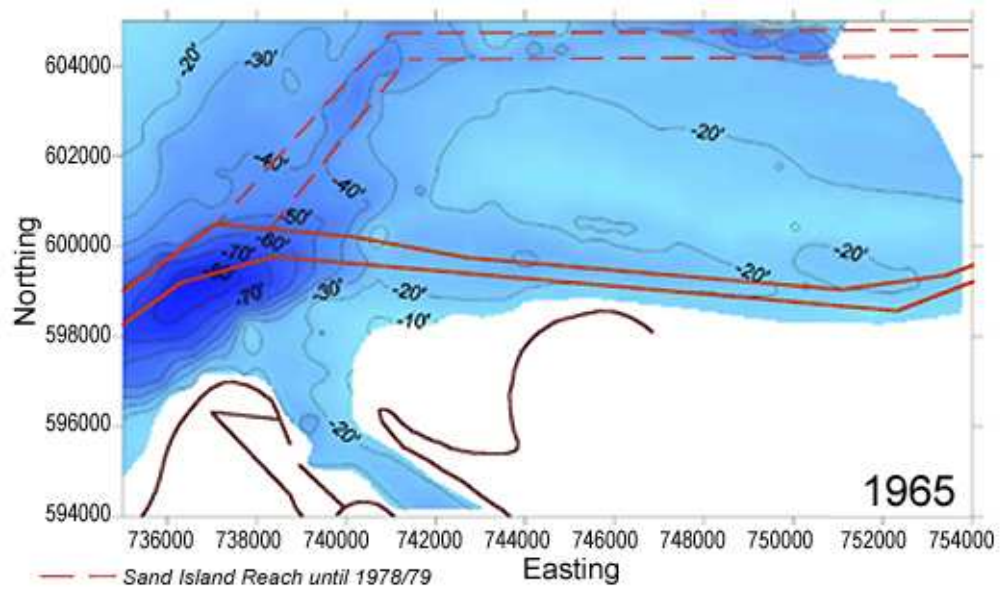


Figure A-2 Bathymetric surface for Grays Harbor main channel in 1965. Depths are feet, mllw.

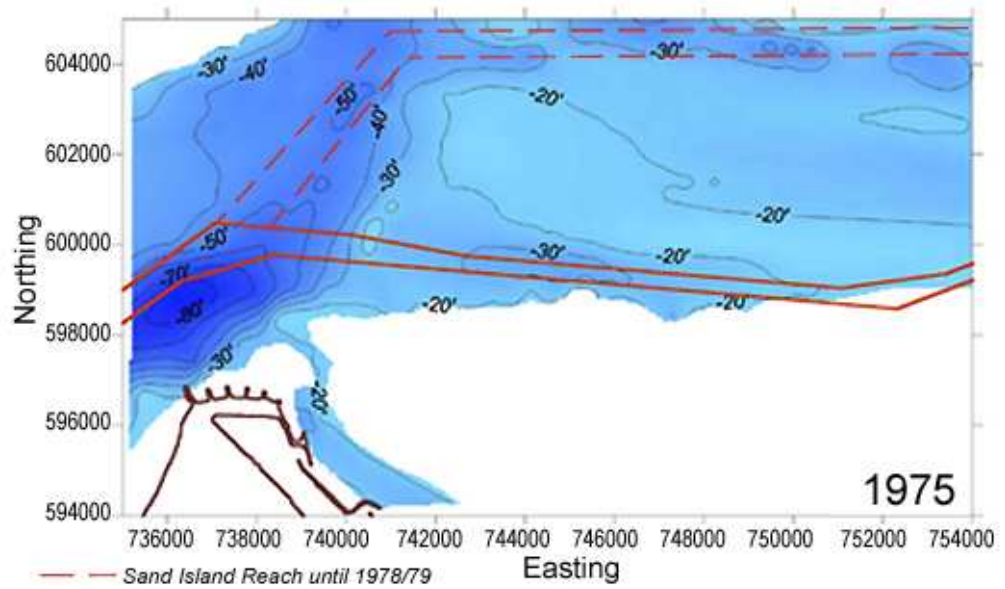


Figure A-3 Bathymetric surface for Grays Harbor main channel in 1975. Depths are feet, mllw.

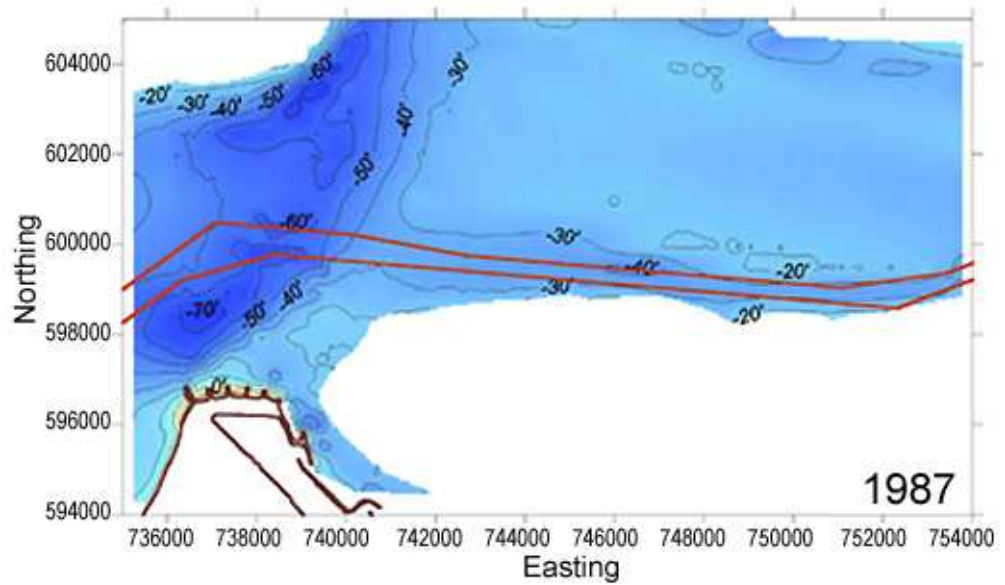


Figure A-4 Bathymetric surface for Grays Harbor main channel in 1987. Depths are feet, mllw.

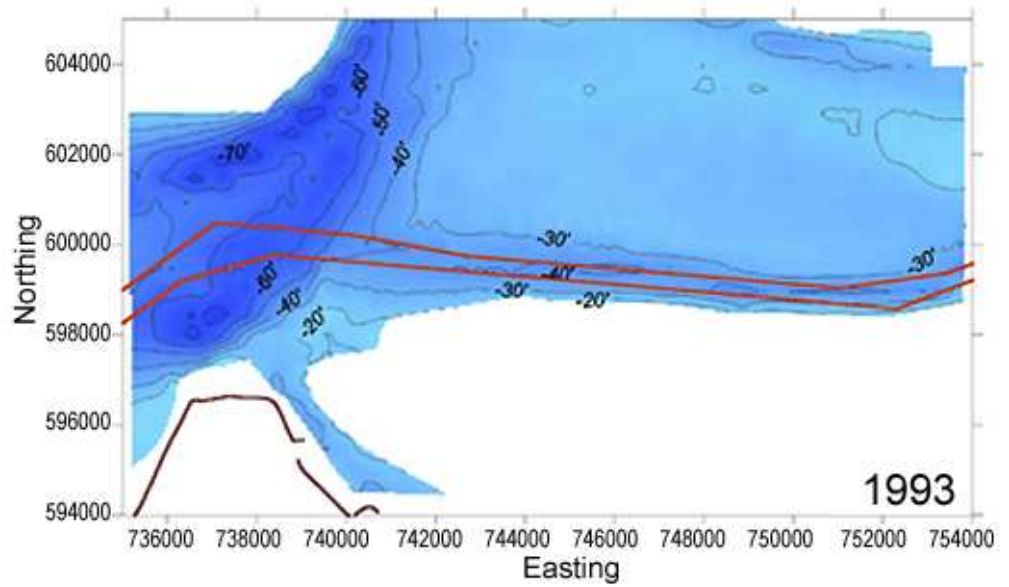


Figure A-5 Bathymetric surface for Grays Harbor main channel in 1993. Depths are feet, mllw.

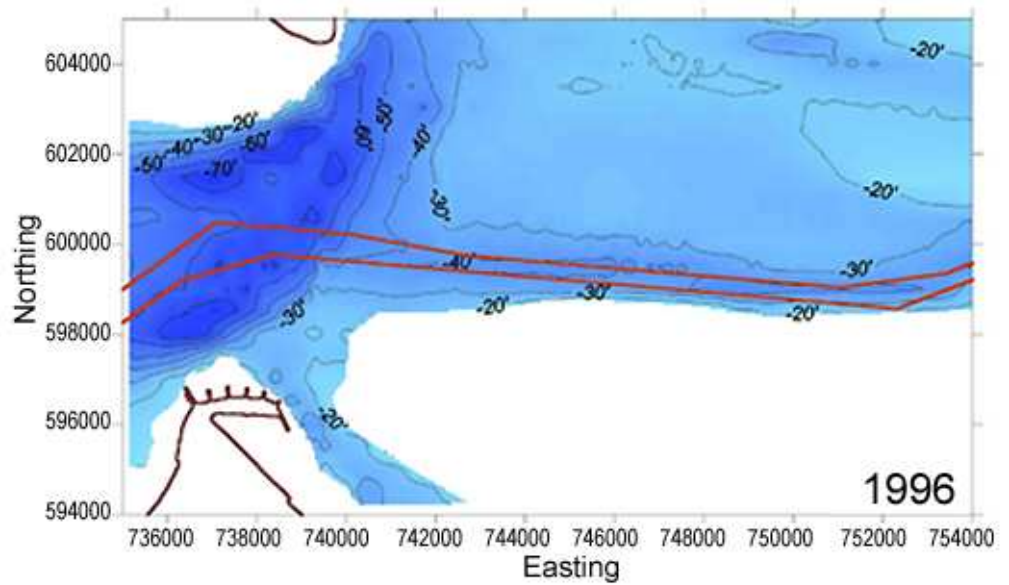


Figure A-6 Bathymetric surface for Grays Harbor main channel in 1996. Depths are feet, mllw.

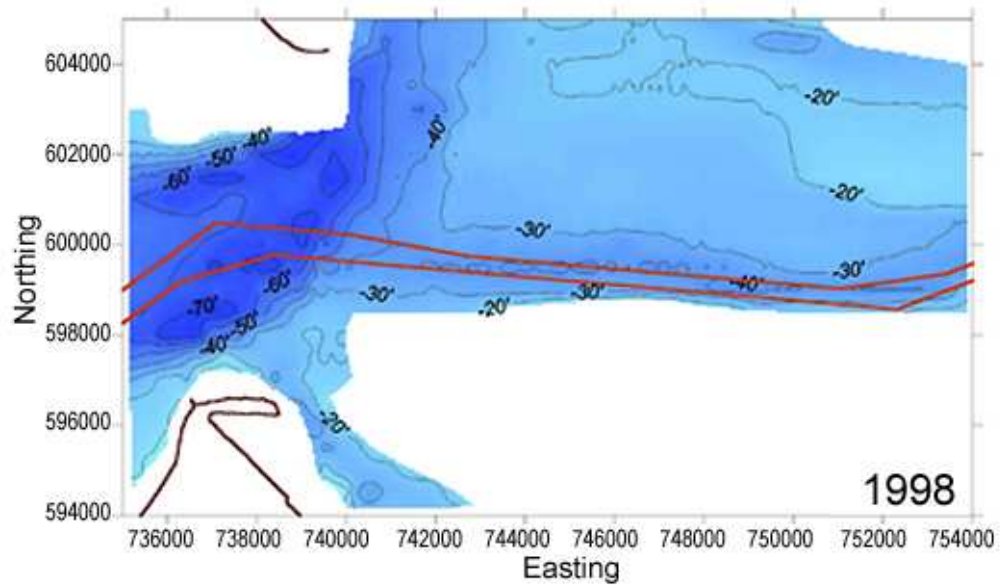


Figure A-7 Bathymetric surface for Grays Harbor main channel in 1998. Depths are feet, mllw.

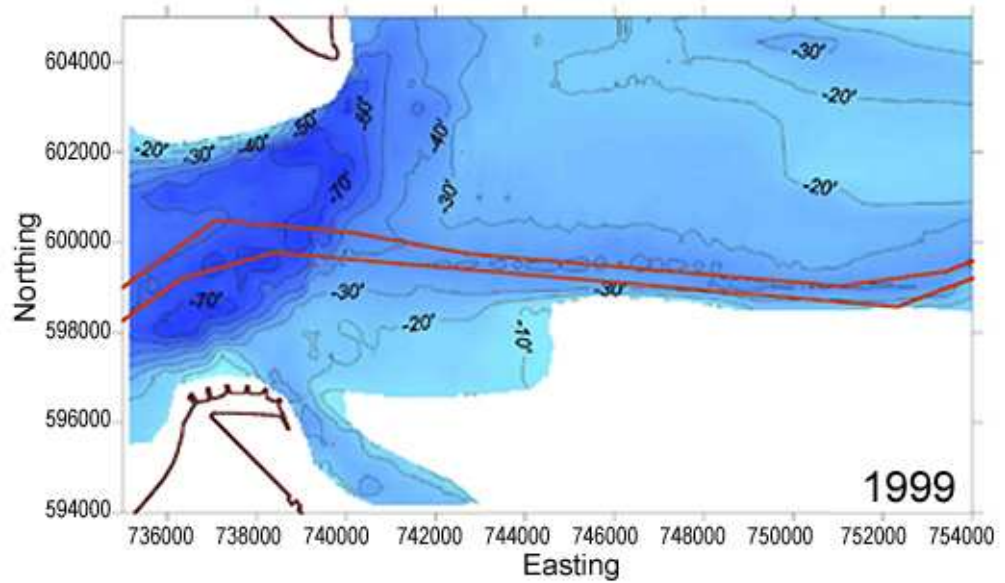


Figure A-8 Bathymetric surface for Grays Harbor main channel in 1975. Depths are feet, mllw.

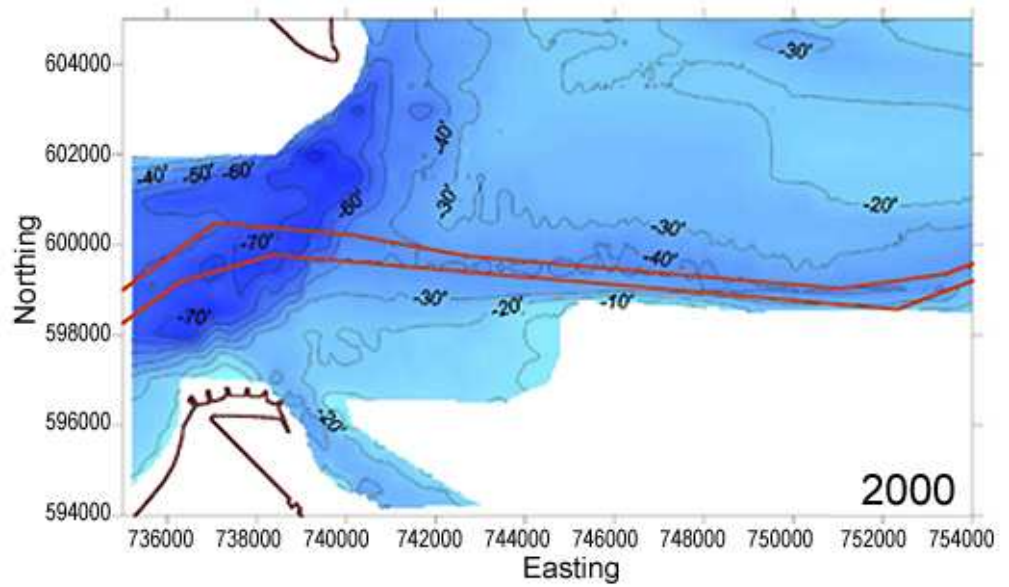


Figure A-9 Bathymetric surface for Grays Harbor main channel in 2000. Depths are feet, mllw.

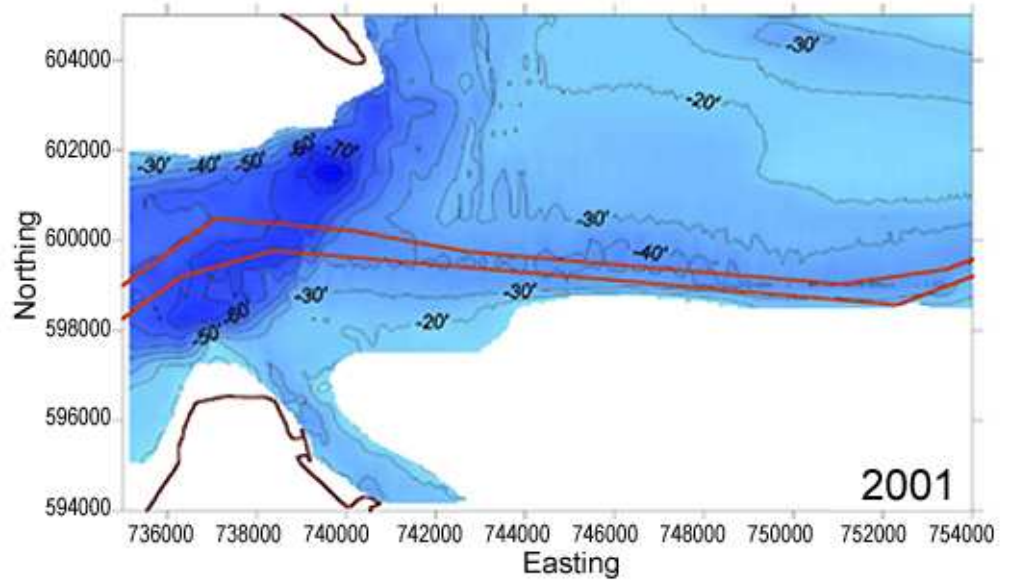


Figure A-10 Bathymetric surface for Grays Harbor main channel in 2001. Depths are feet, mllw.

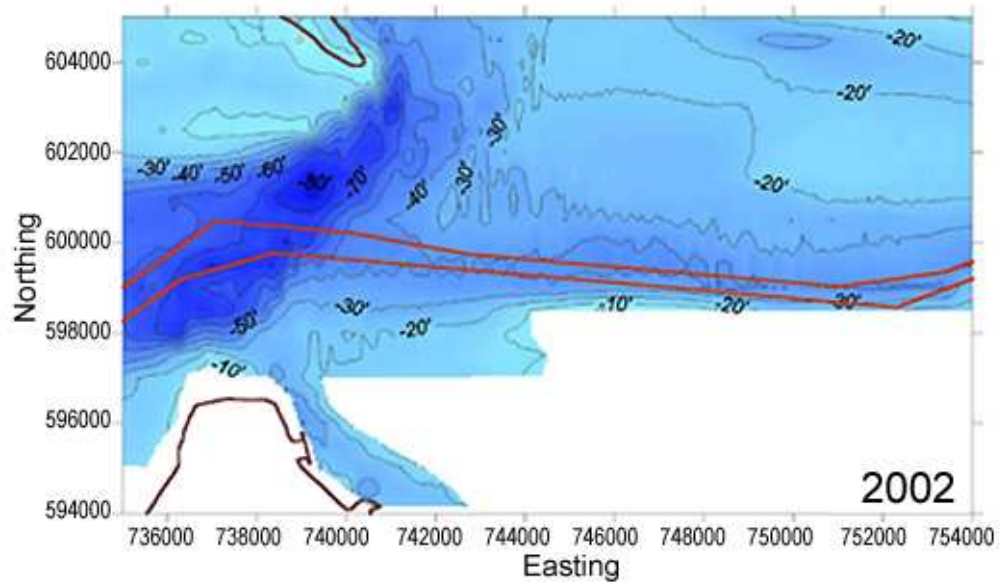


Figure A-11 Bathymetric surface for Grays Harbor main channel in 2002. Depths are feet, mllw.



APPENDIX B.

Combinations of Incident Wave Parameters Simulated with the STWAVE Model.

Table B-1 Combinations of incident wave parameters simulated with the STWAVE model

Wave Direction θ (deg)	Incident Significant Wave Height $H_{s,i}$ (m)	Wave Period T_i (sec)
213.75	1	8
247.50	1	8
270.00	1	8
292.50	1	8
326.25	1	8
213.75	1	12
247.50	1	12
270.00	1	12
292.50	1	12
326.25	1	12
213.75	1	16
247.50	1	16
270.00	1	16
292.50	1	16
326.25	1	16
213.75	1	20
247.50	1	20
270.00	1	20
292.50	1	20
326.25	1	20
213.75	4	8
247.50	4	8
270.00	4	8
292.50	4	8
326.25	4	8
213.75	4	12
247.50	4	12
270.00	4	12
292.50	4	12
326.25	4	12
213.75	4	16
247.50	4	16
270.00	4	16
292.50	4	16
326.25	4	16
213.75	4	20
247.50	4	20
270.00	4	20
292.50	4	20
326.25	4	20
213.75	8	8
247.50	8	8
270.00	8	8
292.50	8	8
326.25	8	8
213.75	8	12
247.50	8	12
270.00	8	12
292.50	8	12
326.25	8	12
213.75	8	16
247.50	8	16
270.00	8	16
292.50	8	16
326.25	8	16
213.75	8	20
247.50	8	20
270.00	8	20
292.50	8	20
326.25	8	20